Adam Mickiewicz University in Poznan

Faculty of Biology

Department of Gene Expression

Uniwersytet im. Adama Mickiewicza w Poznaniu

Wydział Biologii

Zakład Ekspresji Genów

PhD thesis

Rozprawa doktorska

N6 Methyladenosine (m^6A) and its writer mRNA adenosine methylase (MTA) are required for proper miRNA biogenesis in *Arabidopsis thaliana.*

Susheel Sagar Bhat

Poznan, Poland 2020

Poznań, Polska 2020

FUNDING

This work was supported by the following sources:

1. The Polish National Science Centre grants **PRELUDIUM** (**2017/27/N/NZ1/00202)** and **ETIUDA (2019/32/T/NZ1/00122)**
2. The KNOW RNA Research Centre in Poznan **(01/KNOW2/2014)**
3. The European Union: Passport to the future - Interdisciplinary doctoral studies at the Faculty of Biology, Adam Mickiewicz University **(POWR.03.02.00-00-I006/17-00)**

SCIENTIFIC COLLABORATIONS

Scientific experiments were performed at the Department of Gene Expression, Institute of Molecular Biology and Biotechnology, Faculty of Biology, Adam Mickiewicz University, Poznan in collaborations with School of Biosciences, Plant Sciences Division, University of Nottingham, UK; Department of Cellular and Molecular Biology along with Centre For Modern Interdisciplinary Technologies at Nicolaus Copernicus University, Torun and Department of Biology, University of Pennsylvania, USA.

PUBLICATIONS

1. The results discussed in this thesis are presented in a research article titled: "**mRNA adenosine methylase (MTA) deposits m^{6}A on pri-miRNAs to modulate miRNA biogenesis in *Arabidopsis thaliana*"-** under review at PNAS.

Other publications:

1. **Susheel Sagar Bhat**, Dawid Bielewicz, Artur Jarmolowski, Zofia Szweykowska-Kulinska. N6-methyladenosine (m^{6}A): Revisiting the Old with Focus on New, an Arabidopsis thaliana Centered Review. Genes, Dec 2018; 9(12):596. DOI: 10.3390/genes9120596
2. **Susheel Sagar Bhat**, Artur Jarmolowski, Zofia Szweykowska-Kulinska. MicroRNA biogenesis: Epigenetic modifications as another layer of complexity to the microRNA

expression regulation. Acta Biochimica Polonica, Nov 2016, Vol. 63, No 4/2016 717–723; DOI: 0.18388/abp.2016_1370

3. Aleksandra Grabowska, **Susheel Sagar Bhat (shared first author)**, Aleksandra Smoczynska, Dawid Bielewicz, Artur Jarmolowski and Zofia Szweykowska Kulinska. Regulation of plant microRNA biogenesis. In: Miguel C., Dalmay T., Chaves I. (eds) Plant microRNAs. Concepts and Strategies in Plant Sciences. Springer, Cham. Feb, 2020. DOI: /10.1007/978-3-030-35772-6_1
4. Mateusz Bajczyk, **Susheel Sagar Bhat**, Lukasz Szewc, Zofia Szweykowska-Kulinska, Artur Jarmolowski, Jakub Dolata. Novel nuclear functions of Arabidopsis ARGONAUTE1: beyond RNA interference. Plant Physiology. Jan 2019, pp.01351.2018; DOI: 10.1104/pp.18.01351

SUPERVISOR

Prof. dr. hab. Zofia Szweykowska-Kulinska

Department of Gene Expression, Faculty of Biology, Adam Mickiewicz University

Poznan, Poland

ASSISTANT SUPERVISOR

Dr. Dawid Bielewicz

Department of Gene Expression, Faculty of Biology, Adam Mickiewicz University

Poznan, Poland

REVIEWERS

1. Prof. dr hab. Andrzej Dziembowski

   International Institute of Molecular and Cell Biology, Warsaw.
2. Prof. dr hab. Marek Tchórzewski

   Faculty of Biology and Biotechnology, Maria Curie-Skłodowska University, Lublin

ACKNOWLEDGEMENTS

I would like to express my sincere gratitude to Prof. Zofia Szweykowska-Kulinska for giving me a chance to do research under her guidance. Her guidance and support throughout the course of my PhD accompanied by scientific discussions and ideas were instrumental in supporting me during my research.

I would like to thank Dr. Dawid Bielewicz for the immense support, scientific as well as social, during my PhD. The scientific ideas and discussions proved invaluable during my doctoral research.

My sincere thanks to Prof Artur Jarmalowski for the many discussions, ideas and constructive criticisms that helped in shaping the course of my PhD research.

Many thanks to my fellow colleagues and friends especially Łukasz, Halina, Mateusz and Bartek from the Department of Gene Expression for all the scientific discussions and ideas, and for being helpful, supportive and encouraging during my doctoral studies.

This work would not be possible without all the collaborations with people from other labs to whom I would like to convey my sincere thanks.

Last but not the least, thanks to my family and friends without whose support none of this would be possible.

Contents

1. Abstract

The role of miRNAs in post transcriptional gene regulation has been well documented. In plants, miRNAs have been shown to play critical roles in growth and development as well as stress responses. The biogenesis of miRNAs is under various transcriptional and post-transcriptional controls. The processing primary transcripts of MIR genes (primary miRNAs, pri-miRNAs), that carry the miRNA in a stem loop region, is affected by many different processes like splicing, alternative polyadenylation etc. N6A methyladenosine (m^6A) is a well-known RNA base modification that influences RNA metabolism. In plants, m^6A modification is a product of mRNA adenosine methylase (MTA) activity and the lack of MTA/m^6A is embryo lethal for plants, underlying the critical importance of this modification. In this thesis, I investigate whether m^6A modification can also affect miRNA biogenesis in Arabidopsis. I used Arabidopsis line with significantly low expression of MTA (hence m^6A) and discovered that the level of at least 25% of miRNAs in such plants is lower than in wild-type plants whereas the precursors tend to accumulate. Using m^6A targeted RNA immunoprecipitation followed by sequencing I identified 11 pri-miRNAs that carry the m^6A mark. Further, I show that MTA binds to these pri-miRNAs, hence providing evidence for direct methylation of pri-miRNAs by MTA. m^6A is known to alter RNA structure and we tested the secondary structure of pri-miRNAs using Protein Interaction Profile sequencing (PIP-seq). Structural analysis revealed that the pri-miRNAs lose their secondary structures in absence of m^6A. Interestingly, I discover that the binding of HYL1 to pri-miRNAs is also impaired. This may be explained by their distorted structure, since HYL1 is a double stranded RNA binding protein. While investigation the protein-protein interactions of MTA, I found interactions of MTA with Tough (TGH) (a known miRNA biogenesis player) and RNA Polymerase II. I also show that assembly of the Microprocessor complex is impaired in *mta* mutant. These results indicate that MTA acts in early stages of miRNA biogenesis, quite possibly co-transcriptionally. Additionally, I show that by influencing the biogenesis of miR393b (an important regulator of auxin response in plants) MTA/m^6A can affect auxin signalling. The data obtained in this thesis provide first evidence of miRNA biogenesis regulation via m^6A methylation and its writer MTA.

Streszczenie

MikroRNA są kluczowymi regulatorami ekspresji genów na poziomie potranskrypcyjnym. W przypadku roślin stwierdzono, że mikroRNA są istotne w regulacji procesów rozwojowych, jak i odpowiedzi roślin na stresy środowiskowe. Biogeneza mikroRNA jest ściśle kontrolowana zarówno na poziomie transkrypcyjnym, jak i potranskrypcyjnym. Dojrzewanie pierwotnych transkryptów (zwanych pri-miRNA) niosących mikroRNA (zlokalizowane w strukturach typu spinka do włosów) obejmuje wiele dodatkowych procesów, między innymi splicing i alternatywna poliadenylacja. N6-metyloadenozyna (m^6A) jest dobrze znanym modyfikowanym nukleozydem występującym w RNA, pełniącym ważną rolę w kontroli metabolizmu RNA. Katalizę powstania m^6A w RNA przeprowadza enzym zwany metylazą adenozyny mRNA (MTA, ang. mRNA adenosine methylase), a jego brak jest w roślinach embrio-letalny, co podkreśla wagę tego enzymu i modyfikacji m^6A w rozwoju roślin. W przedstawionej pracy doktorskiej zająłem się odpowiedzią na pytanie, czy modyfikacja m^6A jest ważna w biogenezie mikroRNA *Arabidopsis thaliana*. W badaniach wykorzystałem linię transgeniczną *A.thaliana* ze znacząco obniżonym poziomem MTA (a tym samym m^6A) i odkryłem, że w porównaniu do roślin typu dzikiego w roślinach tych poziom około 25% mikroRNA jest znacząco obniżony, czemu towarzyszy akumulacja pri-miRNA. Wykorzystując technikę immunoprecypitacji i przeciwciała skierowane na m^6A, a następnie wysokoprzepustowe sekwencjonowanie kwasów nukleinowych (RIP), zidentyfikowałem 11 pri-miRNA, które zawierały m^6A. Następnie udowodniłem, że MTA oddziałuje z tymi pri-miRNA, tym samym pokazując, że pri-miRNA są substratami MTA. Wiadomo, że obecność m^6A wpływa na strukturę RNA. Przetestowano strukturę drugorzędową pri-miRNA stosując technikę PIP-seq (ang. Protein Interaction Profile sequencing). Analiza wykazała, że zawartość struktur drugorzędowych w pri-miRNA pod nieobecność m^6A znacząco maleje. Dalsze badania pokazały, że wiązanie białka HYL1 z pri-miRNA jest w mutantach *mta* również mocno zaburzone. Wynik ten można tłumaczyć zaburzeniami strukturalnymi, gdyż HYL1 wiąże się z dwuniciowym RNA. Analizując oddziaływania MTA z innymi białkami odkryłem, że MTA oddziałuje z białkiem Tough (TGH), które odgrywa znaczącą rolę w biogenezie mikroRNA. Poza tym stwierdzono, że MTA oddziałuje z polimerazą RNA II. Dalsze analizy wykazały, że białka kompleksu Mikroprocesora (HYL1 i DCL1) kolokalizują niewydajnie w mutantach *mta*

z polimerazą RNA II. Wynik ten wskazuje, że MTA działa na wczesnych etapach biogenezy mikroRNA, najprawdopodobniej kotranskrypcyjnie.

Dodatkowo pokazałem, że zaburzona biogeneza miR393b (cząsteczki ważnej z odpowiedzi roślin na obecność auksyn) w mutancie *mta A. thaliana* zakłóca sygnalizację auksynową.

Wyniki uzyskane w trakcie realizacji niniejszej pracy doktorskiej odkryły kolejny ważny element sieci regulatorowej wczesnych etapów biogenezy mikroRNA – enzym MTA i wprowadzaną przezeń modyfikację – m6A.

2. Introduction

Ribonucleic Acid (RNA), a polymer of ribonucleotides, is often considered to be just an intermediary molecule that participates in vital metabolic processes. These processes, are almost universally directed by the information coded in De-oxy Ribonucleic Acid (DNA) of any given organism. What is worth noting is that DNA could not have evolved without RNA, which essentially means that life as we know it indeed started on the basis of RNA. This is what forms the basis of the theory known as the "RNA world" theory. Proposed in as early as 1960s, the idea that RNA could be at the centre of the evolution of life based on a genetic code is still under active research to this day (for review: Higgs and Lehman, 2015[1]).

Chemically, RNA is a fragile molecule, prone to degradation and mutations, hence life moved on to a more stable DNA based genetic code. Yet, RNA plays a critical role in maintenance of life. Broadly, there exist two classes of RNA: coding and non-coding RNA. While coding RNA (usually messenger RNA; mRNA) is vital for the translation of genetic information from DNA to protein, it is the variety of non-coding RNAs that have control over this translation. RNAs like transfer RNAs (tRNAs) and ribosomal RNAs (rRNAs) are essential for protein production even though they themselves do not carry the protein coding instructions. Then there are various other non-coding RNAs (ncRNAs) further separated into long ncRNAs and short ncRNAs that fine tune the whole cell metabolism by either modifying cellular components like chromatin structure or even directly targeting mRNAs to regulate protein production.

Micro RNAs (miRNAs), as the name suggests, are a sub class of small ncRNAs, that are ~21-24 nucleotide in length. miRNAs were first discovered in *Caenorhabditis elegans*[2–4], later in animals including humans[5]. The first examples of plant miRNAs were reported from the model plant *Arabidopsis thaliana*, as various groups reported the discoveries of abundance of small RNAs in *Arabidopsis*[6–8]. miRNAs are regulatory RNAs that modulate gene expression by specifically targeting a given mRNA. The action of miRNAs results in either a degradation of the target mRNA or an inhibition of translation from the target. The following chapters will take a look on the biogenesis and mode of action of miRNAs in *Arabidopsis.*

2.1 Biogenesis of miRNAs in *Arabidopsis*

Biogenesis of *Arabidopsis* miRNAs starts from *MIR* genes, that are transcribed by RNA Polymerase II (RNA Pol II)[9]. A majority of the *MIR* genes are located in intergenic regions and are transcribed independently[6,7,10]. The Mediator complex (a general transcriptional activator) recruits RNA Pol II to *MIR* genes[11]. *MIR* genes also have an over or under representation of certain promoter elements that provide further specificity to *MIR* gene transcription. TATA box is the most over represented motif in *MIR* genes along with other elements like AtMYC2, G-Box and SORLIP1 elements, while certain *cis*-elements like GATA, LFY and T-box are underrepresented in *MIR* genes as compared to protein genes[9,12,13]. The initial step of transcription by RNA Pol II results in the production of a long precursor (ranging from few hundred to thousand nucleotides[14]) called primary miRNA (pri-miRNA). These pri-miRNAs have the ability to form secondary structures, most notable, a hair-pin loop. This hair-pin loop is critical as the site of cleavage by RNAse III type nuclease Dicer Like 1 (DCL1) is directed by the structural features and the imperfect base pairing at the base of the hair-pin loop[15–19]. This process of first cut at the base of the loop is termed as base to loop processing and is the more prevalent pathway. However, evidence for a loop to base processing, where first DCL1 cut happens towards the loop has also been shown[17]. The decision for a base to loop or loop to base processing is also determined by the secondary structural features of the pri-miRNAs[15]. In a two-step process, DCL1 activity first gives rise to an intermediate precursor miRNA (pre-miRNA) which is again cleaved by DCL1[20]. The pre-miRNAs are just the hair-pin loop part of pri-miRNAs containing the miRNA and its complementary miRNA* (miRNA/miRNA*) in the stem region. Owing to DCL1 activity, pre-miRNAs have 2nt overhangs on the 3' end and a phosphate group at the 5' end. The second cleavage step then releases the miRNA/miRNA* duplex from the pre-miRNAs. The duplex is then methylated on the 3' end by HUA Enhancer 1 (HEN1) which protects the duplex from degradation[21]. Several miRNA/miRNA* duplexes are then exported to the cytoplasm via HASTY (HST) which belongs to the family of importin β nucleocytoplasmic transport receptors[8]. HST is the homolog of animal Exportin 5 protein[8] and although they both are involved in miRNA biogenesis, they both differ in the cargo they export to the cytoplasm. In animals, Exportin 5 exports pre-miRNAs[22–25] which undergo another cleavage in cytoplasm to release miRNA/miRNA* duplexes[26] while HST exports the duplex itself. Finally, the miRNA strand of the miRNA/miRNA* duplex is selectively loaded onto the effector protein of the RNA Induced Silencing Complex (RISC): Argonaute1

(AGO1)[27,28]. Recently, another mechanism of miRNA export was discovered involving AGO1 that will be described later[29].

The process of miRNA biogenesis may seem to be fairly simple at this stage but it is far from that. A myriad of accessory proteins affects all steps of this process starting from transcription to DCL1 activity to the loading of miRNA on AGO1. A pair consisting of Negative on Tata Less 2 (NOT2a) (a member of the Carbon catabolite Repression4 (CCR4)-NOT complex) and NOT2b (Vire2 interacting Protein 2) are positive regulators of *MIR* gene transcription[30]. NOT2b interacts with RNA Pol II as well as DCL1 and other miRNA biogenesis factors and promotes *MIR* gene transcription and recruitment of DCL1. Interestingly, both NOT2a and NOT2b can form homo or hetero dimers and are both necessary for maintaining proper miRNA levels in the cell. Similarly, Cell Division Cycle 5 (CDC5), which is a DNA binding protein also interacts with RNA Pol II and with other proteins including DCL1[31]. Thus, it facilitates RNA Pol II recruitment on *MIR* genes and as well as pri-miRNA processing. Apart from the generalised transcription factors, a variety of conditional transcriptional vectors are also involved in *MIR* gene transcription. Since miRNAs have significant effects on gene expression their production is also under tight control. Depending on environmental cues (biotic or abiotic) or a specific stage of development or an organ, various transcriptional factors can fine tune miRNA biogenesis. For example, in case of phosphate starvation MYB2 transcription factor promotes *MIR399f* transcription and as expected *MIR399* promoter region contains MYB2 binding site and a specific GNATATNC motif that is a known binding site for another transcription factor of the MYB family: Phosphate Starvation Response 1 (PHR1)[32]. *MIR398* family has various stress-responsive elements in their promoter regions like TC- rich regions, low temperature-responsive element (LTR), heat stress-responsive element among others[33]. Notably, Squamosa Promoter Binding Protein-like7 (SPL7) regulates transcription of *MIR398b* and *c* in conditions of copper deficiency[34]. Further, some *MIR* genes can also have specific promoters, as is the case of Apetala 2 (AP2) which promotes *MIR156* transcription but inhibits that of *MIR172*[35].

Post transcriptionally, it is important to note that DCL1 does not process pri-miRNAs in isolation, but does it as a part of a multi protein complex called the Microprocessor[36–38]. Two core members of the Microprocessor, other than DCL1, are a zinc finger protein Serrate (SE)[39,40] and a Double-stranded RNA Binding domain protein 1 (DRB1)[41] [also known as Hyponastic Leaves 1 (HYL1), on account of the phenotype of its mutant]. SE is considered to

bind the pri-miRNAs at the junction of single and double stranded regions while HYL1 binds the double stranded regions as the name DRB1 suggests. Both these proteins are required for the precision of DCL1 cleavage by helping in proper positioning of pri-miRNAs in respect to DCL1 cleavage site. Another protein, Tough (TGH), a G-patch domain protein, also interacts with DCL1, SE and HYL1. It binds the single stranded regions of pri-miRNAs and promotes DCL1 activity without having any influence on its precision[42]. Chromatin Remodelling Factor 2 (CHR2) is an interesting example and worth noting due to its opposing roles in miRNA biogenesis. CHR2 is a member of the SWI/SNF chromatin remodelling complex and on its own positively affects *MIR* gene transcription owing to its ATPase activity. But, upon its association with SE, it remodels pri-miRNAs thanks to its non-canonical RNA helicase activity and the changes in their secondary structures leads to reduction of DCL1 activity and reduced production of mature miRNAs[43].

miRNA/miRNA* duplexes thus released are protected from degradation by 2'-*O*-methylation at their 3' ends by HUA1 enhancer 1 (HEN1). In the absence of this methylation the miRNA/miRNA*duplex is susceptible to degradation mediated by the uridylation of 3' ends of the duplex by HEN1 suppressor 1 (HESO1)[44,45]. Two different pathways regarding the loading of miRNA into AGO1 and formation of functional RISC have been reported so far. First, more traditional pathway, suggests that the methylated duplexes are exported to the cytoplasm via a HST[8]. The loading of miRNA strand into AGO protein takes place in the cytoplasm and the strand selectivity is assisted by HYL1. This model of miRNA/miRNA* export via HST has a couple of weak points. First, in *hst* mutants, the nuclear-cytoplasmic partitioning of miRNAs does not change. Second, HST seems to be more effective in miRNA export in regards to certain miRNAs and tissue[8]. These issues in the traditional pathway can be partially explained by a recent report that provides evidence of RISC assembly happening in the nucleus. In their report, the authors show that AGO1 possess' both a nuclear localization and nuclear export signal (NLS and NES). AGO1 in the nucleus can be loaded with miRNA and then exported to the cytoplasm as AGO1:miRNA complex[29]. Interestingly, AGO1 has also been shown to be associated with the chromatin especially under salt stress[46], which makes it even more likely that miRNA loading to AGO1 could take place in the nucleus. **Fig. 1** summarizes all events that take place during miRNA biogenesis in plants.

2.2 miRNA guided gene regulation

Irrespective of the place where miRNA is loaded on AGO1, the RISC formed as a result, acts in the cytoplasm. RISC induced post-transcriptional gene regulation can be a result of either the cleavage or translational inhibition of the target mRNA. Whether a mRNA will be cleaved or its translational will be inhibited depends on the degree of complementarity between the miRNA and mRNA. Plant miRNAs are usually highly complementary to their target mRNAs[47] and hence cleavage of the target mRNA is the dominant outcome of miRNA action. The PIWI domain in AGO proteins is responsible for the target cleavage while DRB3/5 facilitate this process[48–52]. The cleavage products are then degraded by a variety of nucleases including Exoribonuclease 4 (XRN4)[53], RISC Interacting Clearing 3'-5' Exoribonuclease 1 (RICE1)[54] and cytoplasmic exosome subunits like Superkiller 2 (SKI2), SKI3 and SKI8[55].

Translational repression of the target mRNA is an infrequent path for miRNA action in plants. Only a small number of miRNA targeted mRNAs are translationally repressed. Translational repression is usually caused by the hindrance in ribosome binding to mRNA caused by RISC. miR172 and miR156/7 cause translational repression of their targets, Apatela 2 (AP2) and Squamosa Protein Binding Protein-Like 3 (SPL3), respectively[56,57]. Many accessory proteins like DRB2[58], Katanin 1 (KTN1)[59,60] and Altered Meristem Program 1 (AMP1) are linked to the translational repression process. It is also possible that some miRNA may regulate gene expression both by target cleavage and translational repression.

Apart from post-transcriptional gene regulation, miRNAs have also been demonstrated to regulated gene expression on transcriptional level. DCL3 dependent, 24nt long miRNAs that associate with AGO4 have been shown to direct cytosine DNA methylation of both *MIR* and target genes[61,62].

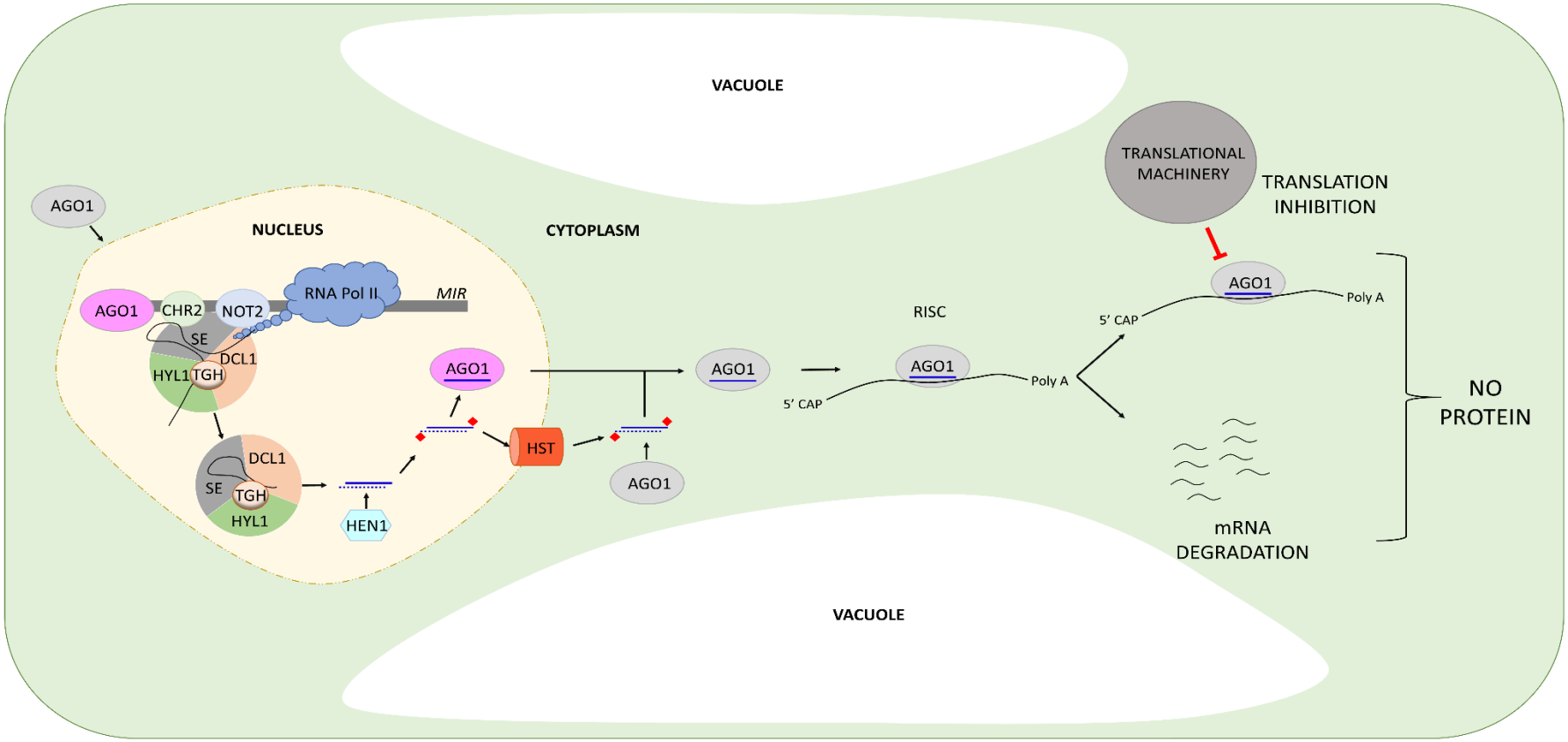

Figure 1. miRNA biogenesis in plants: RNA Pol II transcribes MIR genes to produce hairpin containing pri-miRNAs. NOT2 is a transcriptional factor while CHR2 is an ATPase that positively influence this transcription. Pri-miRNAs are processed in a two-step process by a multi protein complex called Microprocessor (DCL1, SE and HYL1). TGH is necessary for bringing HYL1 to the precursor but is not yet considered to be a bona fide member of Microprocessor. After the miRNA/miRNA* duplex (represented by a pair of solid/dashed lines) is released by the Microprocessor, it is methylated by HEN1 on 3' ends (red diamonds). The miRNA strand is then loaded into AGO1 (nuclear fraction in pink) or exported via HST. In the cytoplasm, AGO1 loaded with miRNA binds to target mRNA and causes either degradation or translational inhibition of the target. AGO1 association with chromatin has also been demonstrated under salt stress.

2.3 Roles of miRNAs in plant sustenance

miRNAs are small entities but they are big influencers of plant development, growth and stress responses. Starting from as early as embryo development, miRNAs are active in shaping plant growth and development. miR165/166 target the class III homeodomain leucine zipper (HD-zip) family of genes, Phabulosa (PHB), Phavoluta (PHV) and Revoluta (REV)[63,64]. These genes play significant role in early embryogenesis, especially in the control of organ polarity. miR394 is necessary for maintenance of Shoot Apical Meristem (SAM) and regulates stem cell competence[65]. miR171a controls Hairy Meristem 1 (HAM1) expression at the level of a single cell layer and regulates proper embryogenesis[66]. Similarly, Cup Shaped Cotyledon 1 and 2 (CUC1/2), that play vital role in organ boundary formation and SAM initiation, are targeted by miR164 for proper regulation of expression[67–69]. In the later stages of development, miR172 and miR159 regulate flower development via targeting Apatela 2 (AP2) and MYB transcription factors MYB33 and MYB65, respectively[56,70]. miR156 and its target Squamosa Promoter Binding Protein Like (SPL) regulate the switch from juvenile to adult phase in plants[71]. miR165/166 regulates vascular development[72], miR857 and miR397b both are involved in lignin biosynthesis regulation[73]. These are a few examples of various miRNAs and the role they play in vital developmental processes in plants.

miRNAs are also involved in plant signalling pathways, especially auxin signalling. miR393 regulates Transport Inhibitor Response 1 (TIR1)/Auxin Signalling F-box Protein 2 (AFB2) that are essential for auxin dependent developmental pathways[74–76]. Similarly, miR160 and miR164 influence auxin signalling dependent plant development via their targets Auxin Response Factor 17 (ARF17) and NAC domain containing protein 1 (NAC1), respectively[77,78]. Secondary metabolite pathways are also affected by miRNAs. miR156-SPL9 pair is involved in terpenoid and flavonoid synthesis in *Arabidopsis*[79,80]. miR858a targeted R2R3-MYB transcription factor affects flavonoid biosynthesis[81]. miR826 and miR5090 target Alkenyl Hydroxyalkyl Producing 2 (AOP2) and negatively impacts glucosinolate biosynthesis[82].

Apart from various aspects of growth and development, miRNAs also regulate plant response to both biotic and abiotic stresses[83]. miR169 regulated Nuclear Factor Y subunit A5 (NFYA5) provides drought tolerance[84], miR393, miR160 and miR167 are upregulated during drought or salinity stress. miR168 is upregulated during cold stress and miR168 targets AGO1 transcripts. The homeostasis between mir168/AGO1 is also affected by abscisic acid stress and drought stress[85], thus changes in miR168 levels can affect many different targets indirectly.

miR160 and miR159 play vital roles in heat tolerance via ARFs and MYB transcription factors. These are just a few examples among the myriad of miRNAs whose expression is changed in response to stress and these changes either help the plants to cope with the stress or sometimes make it more vulnerable.

2.4 m^6A methylation and the related protein players

RNA modifications are fairly common and more than 150 different types of these have been reported so far. Apart from the cap and tail modifications, that are trademark for most RNAs transcribed by a particular RNA Polymerase, internal modifications add more complexity to the RNA molecules. In case of plant mRNAs the following internal modifications have been identified so far: methylation of Adenosine (m^7G, m^6A and m^1A), methylation of Cytosine (m^5C, hm^5C) and uridylation[86]. Among these, methylation of adenosine at nitrogen-6 position (m^6A) is generally considered to be the most abundant internal RNA modification abundant across Eukaryota, and is found not only in mRNA but also, tRNA, rRNA and other ncRNAs[89]. m^6A was first discovered in maize and wheat in 1979[90,91] and much more recently in *Arabidopsis* (2008)[92]. A recent renaissance regarding the investigation of m^6A was fuelled by technological advances and development of new methods and techniques. Previously, functional studies to investigate m^6A and its role in RNA metabolism remained challenging as it does not change the Watson-Crick base pairing and hence could not be detected by traditional reverse transcription methods.

m^6A is a reversible modification which is deposited on RNA by a multi protein methyl transferase complex on an adenosine within a specific sequence motif of RRACH (R = G/A, H = A/C/U)[93]. The complex consists of various proteins, most notably three core members called mRNA m^6A methyl transferase A (MTA)[92], mRNA m^6A methyl transferase B (MTB)[94] and FKBP12 interacting protein 37 kDa (FIP37)[92,95]. MTA is the catalytic component of the methyl transferase complex although it has been noted that all three components are needed for high activity. All three components are essential for plant viability, pointing towards the critical role of these proteins and m^6A in plant survival. MTA has been shown to be highly expressed in actively dividing tissue and its expression pattern corresponds to that of m^6A levels[92]. Not much is known about MTB except its embryo lethality and direct interactions with the components of the m^6A methyl transferase complex[94]. FIP37 was the first protein partner of MTA to be identified and shares expression patterns with the latter. It is critical for maintenance of shoot

apical meristem[95]. As knockout of any of these three proteins is embryo lethal, studies focusing on the role of these proteins use similar strategies wherein the proteins are expressed at required levels in embryonic development and at very low levels in the later stages. This is achieved using specialised embryo specific promoters, usually *ABI3*[92].

Apart from MTA, MTB and FIP37, other proteins have been identified as a part of the m^6A methyl transferase complex. A splicing factor Virilizer (*At*VIR) has been shown to interact with the components of the m^6A methyl transferase complex. Knockout of *At*VIR is also embryo lethal and lower levels of *At*VIR also result in lower m^6A levels. Another protein, HAKAI has been identified as an interactor and part of the m^6A methyl transferase complex proteins. Although, interestingly, in contrast to other members, complete knockout of HAKAI does not result in any obvious phenotypical defects, even though m^6A levels are lower in such plants[94].

As mentioned earlier, m^6A is a reversible modification. This implies the existence of proteins that remove this modification from the RNA. These proteins are called m^6A 'erasers'. In *Arabidopsis,* 13 members of a group thought to have 'eraser' activity exist. These proteins belong to the AlkB family of non-heme Fe(II)/α-ketoglutarate (α-KG)-dependent dioxygenases family proteins and their homologs (ALKBH). 2 out of these 13, ALKBH9B and ALKBH10B, have been experimentally shown to be actively involved in m^6A removal[96,97]. ALKBH9B acts on viral ssRNAs to demethylate them and in its absence hyper methylated viral RNA is degraded[96]. ALKBH10B plays a role in the flowering time as its activity modulates degradation of mRNA for a flowering locus T (FT) mRNA[97]. In addition to the 'writers' and the 'erasers', another class of proteins called the 'readers' have been described in relation to the m^6A modification. These 'reader' proteins identify the m^6A mark and are usually the starting points in a reaction cascade that eventually leads to the observable metabolic affects attributed to m^6A methylation. YT521-B homology (YTH) domain family proteins (two clades are present: DF (YTHDF) and DC (YTHDC)) belong to the 'reader' class. In Arabidopsis, Evolutionarily Conserved C-Terminal Region (ECT) proteins contain the YTH domain and so far, 13 such proteins have been identified[89]. ECT2 protein has been functionally shown to increase the stability of m^6A modified RNAs involved in trichome morphogenesis[98–100]. A large pool of 'erasers' and 'readers' still await investigation.

2.5 Roles of m^{6}A in plant growth and development

As mentioned earlier, complete lack of m^{6}A in plants is embryo lethal which indicates towards the vital roles this modification plays in plant sustenance. A reduced level of m^{6}A leads to visible phenotypic defects in plants. These defects include shorter inflorescences, changes in flower morphology, increased trichome branching, hampered auxin signalling, and reduced seed production[92,94]. These defects are usually a result of the changes in RNA structure or metabolism caused by lack of m^{6}A. Depending on the detection of m^{6}A in particular mRNAs, it is suggested that m^{6}A can also play a role in physiological processes like photosynthesis[93] and alkaloid synthesis[101]. As mentioned earlier, m^{6}A demethylase, ALKBH9B demethylates viral RNA, thus showing that m^{6}A is also important for plant stress response to biotic stress[96]. m^{6}A reader proteins ECT1 and ECT2 interact with Calcineurin B-Like-Interacting Protein Kinase1 (CIPK1), which in turn is important in calcium signaling pathway[102].

The varied ways by which m^{6}A affects RNA metabolism are mostly known for mRNAs and more so for animal mRNAs. In animals, m^{6}A methylation is regarded as a signal for mRNA decay on a global level[103,104]. But that is not all, m^{6}A also influences mRNA splicing[105–107], alternative poly-adenylation[108,109], and promotes mRNA export[110,111] as well as translation[112–115]. In plants, m^{6}A has been shown to have a globally stabilizing effect on mRNAs by inhibiting their cleavage[116]. Exceptionally, Shootmeristemless (STM) and Wuschel (WUS) mRNAs, that are critical for proper maintenance of Shoot Apical Meristem (SAM), were shown to be marked for degradation by m^{6}A[93]. The m^{6}A demethylase ALKBH10B targets FT, SPL3 and SPL9 mRNAs for demethylation and these mRNAs are also more stable in the absence of m^{6}A[97]. Whether plant mRNA export, splicing and translation is also affected by m^{6}A remains to be investigated. The majority of these stabilizing/destabilizing effects are result of binding of reader proteins to the m^{6}A mark. A reader protein ECT2 has been shown to provide stability to m^{6}A modified mRNAs[100]. Research showing the inhibition of ribonucleolytic cleavage by m^{6}A also shows that the m^{6}A-regulated cleavage areas are often enriched in U-rich sequences[116]. HNRNP class of reader proteins is known to bind U rich sequences around the m^{6}A modification[117]. As a result of m^{6}A affecting the fundamentals of RNA metabolism, its effects on the overall cellular functions is much more compounded. With the field gaining momentum only recently, many more functions of m^{6}A will be unveiled in greater detail.

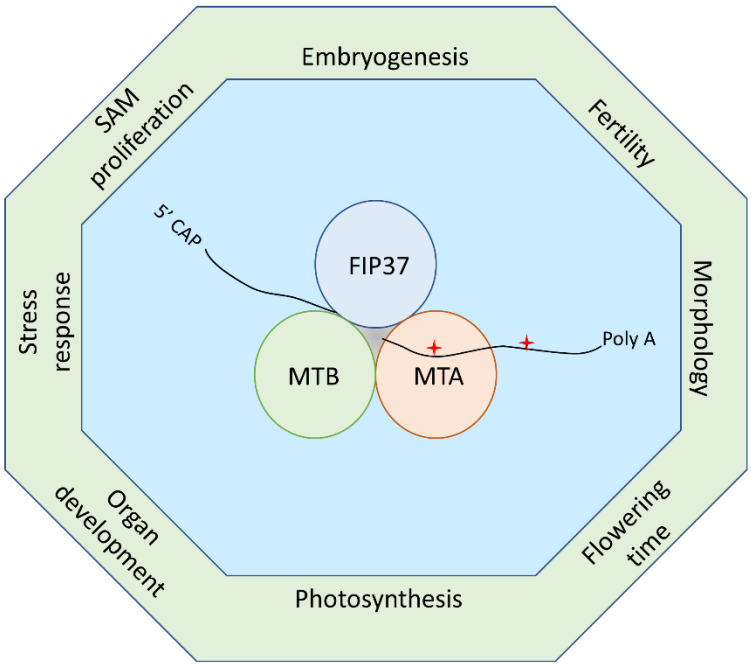

Figure 2. m^{6}A writers and its functions: The core methyl-transferase complex consists of MTA, FIP37 and MTB. MTA is the catalytic subunit that methylates adenosine within a consensus RRACH (R = G/A, H = A/C/U) sequence. m^{6}A methylation is marked by 4 pointed stars. m^{6}A has been shown to influence various vital metabolic processes like embryogenesis, fertility, SAM proliferation, stress response, photosynthesis, etc.

3. Aim of the study

miRNAs are vital cogs in the cellular machinery, necessary for its proper functioning. Similarly, m^6A is a crucial modification that has the ability to shape the cellular landscape. Since m^6A is such a global RNA modification, it is very likely that it also has an influence on the miRNA biogenesis in *Arabidopsis.* The aim of this study was to dig deeper into this co-relation and identify whether

- the presence or absence of m^6A can alter the miRNA biogenesis in *Arabidopsis*
- the observed changes (if any) in miRNA biogenesis are a result of direct action of m^6A writer MTA
- MTA can affect miRNA biogenesis via its interactions with other miRNA biogenesis related proteins
- any physiological changes seen in *mta* hypomorphic mutant can be attributed directly to the interplay between m^6A and miRNA biogenesis pathway

We hypothesized that:

MTA could influence miRNA biogenesis as a direct consequence of m^6A methylation and/or via interactions with other miRNA biogenesis related proteins.

4. Materials and methods

4.1 Materials

4.1.1 Plant material and growth conditions

Arabidopsis thaliana (L.) Heynh accession Columbia-0 (Col-0) was used as the wild type and a transgenic line with FLAG tagged GFP line was used as control for MTA-GFP line. Hypomorphic mutant plants of MTA (*mta),* a transgenic line expressing MTA tagged with GFP under 35S promoter and *mta* mutant with *proDR5:GUS* were obtained from the lab of Dr. Rupert Fray, University of Nottingham, United Kingdom. A homozygous T-DNA insertion line *tgh-1* (SALK_053445) was also used. All *Arabidopsis* plants were grown on Jiffypots® and stratified for 2 days in dark at 4°C. Thereafter, the plants were grown in plant growth chambers at 22°C with 16h light and 8h dark cycles (50–60% humidity, 150–200 $\mu molm^{-2}$ s^{-1} photon flux density). Rosette leaves from 4 weeks old plants were harvested, immediately flash frozen in liquid nitrogen and used, or stored at -80°C until further use.

Nicotiana benthamiana wild type plants were used for transient expression experiments. These plants were grown in sterile soil in an MLR-350H Versatile Environmental Test Chamber (Sanyo, UK) with a 16-h day (approx. 150-200 µE/m2), a constant temperature of 25°C, and 60% humidity.

4.1.2 Bacterial strains and growth conditions

Escherichia coli strains DH5α and DB3 were used for cloning and plasmid amplification. *E. coli* were grown in Luria-Bertini liquid or solid (1.5% Agar) medium at 37°C (with shaking for liquid culture). *Agrobacterium tumefaciens* strain AGL1 was used for expression of shuttle vectors and transformation of *Arabidopsis thaliana* as well as transient expression in *Nicotiana benthamiana. A. tumefaciens* was grown at 28°C (with shaking for liquid cultures).

4.1.3 Yeast strain and growth conditions

Saccharomyces cerevisiae yeast strain Y2HGold was used for the investigation of protein-protein interactions. Yeast was propagated at 28°C on 1x YPDA medium. After transformation

yeast was grown on synthetically defined medium (SD) lacking essential amino acids depending on the selection criteria.

4.1.4 Vectors

The following table lists the vectors and their experimental uses

VECTOR	USE
pGADT7	Yeast Two Hybrid, Activation Domain
pGBKT7	Yeast Two Hybrid, Binding Domain
pENTR™/D-TOPO®	Entry vector for gateway cloning
pMDC32	Gateway destination vector (protein expression)
pSU3/pSU5	Gateway destination vectors (microscopy)

4.1.5 Buffers and solutions

1. LB (Luria-Bertani) medium

LB medium was prepared as follows:

A solution of 1% bactotryptone (BioShop), 0.5% yeast extract (BioShop) and 1% NaCl (Sigma) was autoclaved at 121°C for 20 min under 1 atm pressure. Autoclaved media was cooled to approx. 50°C before the appropriate antibody was added.

For preparing LB solid medium an additional 1.5% bacterial grade agar (BioShop) was added to the mix before autoclaving. After addition of antibiotic the medium was poured in sterile petri dishes and left to solidify for 20-25min. Plates with media were stored at 4°C and used within one month.

2. Antibiotic solutions

ANTIBIOTIC	STOCK CONCENTRATION	WORKING CONCENTRATION
Ampicillin	50mg/ml	50µg/ml
Kanamycin	50mg/ml	50µg/ml

3. RNA and DNA analysis

RNAse free water: 1ml Diethyl pyrocarbonate (DEPC) (Sigma) was added to 1l of milliQ water and incubated overnight at RT. The solution was then autoclaved twice at 121°C for 20 min at 1 atm. pressure.

10X TBE buffer: 10X TBE stock was prepared with the following composition

0.89M Tris base (Sigma)

0.89M Boric acid (Sigma)

0.02M EDTA (Thermo Scientific)

The solution was autoclaved (121˚C, 1 atm., 20 minutes) and stored at RT.

Agarose gel: To prepare agarose gel 1-2% of w/v agarose (Prona Agarose) was dissolved in 1X TBE and boiled in a microwave till agarose dissolved completely. The solution was cooled to ~50°C and Ethidium Bromide (EtBr, Sigma) was added to a final concentration of 0.05mg/100ml). The solution was poured into a casting tray with a comb and let to set for at least 20 min.

RNA loading buffer: To prepare 2X RNA loading buffer, the following recipe was used

0.01M Tris·HCl pH 7.5 (Sigma)

2.5 mM EDTA (Thermo Scientific)

95% Formamide (Sigma)

0.01% Xylencyanol (Sigma)

0.01% Bromophenol blue (Sigma)

The solution was prepared in DEPC treated water and mixed properly before aliquoting in 2ml tubes and stored at -20°C till further use.

DNA loading buffer (2x HSE): To prepare 2x HSE, the following recipe was used

4 M Urea (Sigma)

50% Sucrose (Sigma)

0.05M EDTA (Thermo Scientific)

0.1% Xylencyanol (Sigma)

0.1% Bromophenol blue (Sigma)

The solution was stored at -20°C for long term storage and RT for short term use.

10% SDS solution: 10% Sodium Dodecyl Sulfate (w/v) was dissolved in milliQ water and filtered using 0.22µm syringe filters (Millipore). Solution was stored at RT.

10% APS solution: Ammonium peroxydisulfate (10% w/v) was dissolve in milliQ water and filtered using 0.22µm syringe filters (Millipore). Solution was aliquoted and stored at -20°C till further use.

Saline Sodium Citrate buffer SSC (20x)**:** The following ingredients were dissolved in DEPC treated water

3M NaCl (Sigma)

0.34M Sodium Citrate (Sigma)

The solution was autoclaved (121˚C, 1 atm., 20 minutes) and stored at RT.

Hybridization buffer: Hybridization buffer was prepared by making the following solution using DEPC treated water

0.375M Na_2HPO_4 (Sigma)

125 mM NaH_2PO_4 (Sigma)

1% SDS (BioShop)

The solution was filtered using 0.45µm filters (Millex-HP) and stored at RT.

4. m^6A immunoprecipitation buffers

NP-40: 10% solution of NP-40 detergent (w/v) was prepared in DEPC treated water. The solution was filtered using 0.22µm syringe filter (Millipore) and stored at RT.

Low Salt buffer (LSB): To prepare LSB, the following ingredients were used

0.05M NaCl (Sigma)

0.01M Tris-HCl, pH 7.5 (Sigma)

The solution was autoclaved (121˚C, 1 atm., 20 minutes) and stored at RT.

High Salt Buffer (HSB): To prepare HSB, the following ingredients were used

0.5M NaCl (Sigma)

0.01M Tris-HCl, pH 7.5 (Sigma)

The solution was autoclaved (121˚C, 1 atm., 20 minutes) and stored at RT.

IP buffer: To prepare IP buffer, the following ingredients were used

0.15M NaCl (Sigma)

0.01M Tris-HCl, pH 7.5 (Sigma)

The solution was autoclaved (121˚C, 1 atm., 20 minutes) and stored at RT.

5. RNA Immunoprecipitation buffers

Phosphate Buffer Saline (PBS): To prepare 10X PBS, following recipe was used

1.3M NaCl (Sigma)

0.03M Na2HPO4.H2O (Sigma)

0.03M NaH2PO4.7H2O (Sigma)

The solution was prepared in DEPC treated water and autoclaved (121˚C, 1 atm., 20 minutes) and stored at RT.

Glycine: 2M glycine (Sigma) solution was prepared using DEPC treated water, autoclaved (121˚C, 1 atm., 20 minutes) and stored at RT.

Phenylmethanesulfonyl fluoride (PMSF): 2M solution of PMSF (Sigma) was prepared in iso-propanol. Stored at RT.

Nuclei Isolation Buffer I: To prepare Nuclei isolation buffer I a solution with the following sterile reagents in given working concentrations was made in DEPC water and stored at 4°C till further use.

0.01M Tris HCL, pH 8 (Sigma)

0.01M $MgCl_2$ (Sigma)

0.4M Sucrose (Sigma)

Before use, β-mercaptoethanol (final concentration: 0.035% v/v; Sigma) and phenylmethanesulfonyl fluoride (PMSF, final concentration 0.001M) was added to the buffer.

Nuclei Isolation Buffer II: To prepare Nuclei isolation buffer II a solution with the following sterile reagents in given working concentrations was made in DEPC water and stored at 4°C till further use.

0.01M Tris HCL, pH 8 (Sigma)

0.01M $MgCl_2$ (Sigma)

0.4M Sucrose (Sigma)

1% Triton X-100 (Sigma)

Before use, β-mercaptoethanol (final concentration: 0.035% v/v; Sigma), Complete EDT free protease Inhibitor (0.02 tab/ml; Sigma) and phenylmethanesulfonyl fluoride (PMSF, final concentration 0.001M) was added to the buffer. Additionally, RNAseIn Plus RNAse inhibitor (Promega) was added to the solution in concentration of 80U/ml.

Nuclei Isolation Buffer III: To prepare Nuclei isolation buffer III a solution with the following sterile reagents in given working concentrations was made in DEPC water and stored at 4°C till further use.

0.01M Tris HCL, pH 8 (Sigma)

0.002M $MgCl_2$ (Sigma)

1.7M Sucrose (Sigma)

0.15% Triton X-100 (Sigma)

Before use, β-mercaptoethanol (final concentration: 0.035% v/v; Sigma), Complete EDT free protease Inhibitor (0.02 tab/ml; Sigma) and phenylmethanesulfonyl fluoride (PMSF, final concentration 0.001M) was added to the buffer. Additionally, RNAseIn Plus RNAse inhibitor (Promega) was added to the solution in concentration of 160U/ml.

Sonication buffer: To prepare the sonication buffer, the following reagents were mixed in the given concentrations.

10% Sucrose (Sigma)

0.1M Tris–HCl, pH 7.5 (Sigma)

0.005M EDTA (Sigma)

0.005M EGTA (Sigma)

0.3M NaCl (Sigma)

0.75% Triton X-100 (Sigma)

0.15% SDS (BioShop)

0.001M Dithiothreitol (DTT) (Sigma)

Buffer was made in DEPC treated water and stored at 4°C. Before use, buffer was supplemented with 160U/ml of RNAseIn Plus RNAse inhibitor (Promega).

Low Salt buffer: To make the low salt buffer a solution with the reagents in the following final concentrations was prepared.

0.02M Tris HCl pH8 (Sigma)

0.002M EDTA (Sigma)

1% Triton X-100 (Sigma)

0.15M NaCl (Sigma)

0.1% SDS (BioShop)

The buffer was prepared in DEPC treated water and stored at 4°C

High Salt buffer: To make the high salt buffer a solution with the reagents in the following final concentrations was prepared.

0.02M Tris HCl pH8 (Sigma)

0.002M EDTA (Sigma)

1% Triton X-100 (Sigma)

0.5M NaCl (Sigma)

0.1% SDS (BioShop)

The buffer was prepared in DEPC treated water and stored at 4°C

Lithium Chloride (LiCl) buffer: To make the LiCl buffer a solution with the reagents in the following final concentrations was prepared.

0.01M Tris HCl pH8 (Sigma)

0.002M EDTA (Sigma)

0.25M LiCl (Sigma)

1% NP-40 (Sigma)

1% Sodium deoxycholate (Sigma)

The buffer was prepared in DEPC treated water and stored at 4°C

TE buffer: To make the TE buffer a solution with the reagents in the following final concentrations was prepared.

0.01M Tris HCl pH8 (Sigma)

0.001M EDTA (Sigma)

The buffer was prepared in DEPC treated water and stored at 4°C

IP buffer: To make the IP buffer a solution with the reagents in the following final concentrations was prepared.

0.05M HEPES pH 7,5 (Sigma)

0.15M NaCl (Sigma)

10μM $ZnSO_4$ (Sigma)

1% Triton X-100 (Sigma)

0.05% SDS (BioShop)

Before use, Complete EDT free protease Inhibitor (0.02 tab/ml; Sigma) and phenylmethanesulfonyl fluoride (PMSF, final concentration 0.001M) was added to the buffer. Additionally, RNAseIn Plus RNAse inhibitor (Promega) was added to the solution in concentration of 160U/ml.

RIP elution buffer: RIP elution buffer was prepared containing the following reagents in given final concentrations

0.01M Tris HCl pH8 (Sigma)

0.001M EDTA (Sigma)

1% SDS (BioShop)

The buffer was stored at RT.

6. Yeast Two Hybrid buffers and media

Glucose: 40% w/v glucose (Sigma) was prepared in milliQ water and filtered using 0.45µm filters (Millex-HP). Solution was stored at RT.

YPDA medium: To prepare YPDA medium the following solution was made.

2% Peptone (BioShop)

1% Yeast extract (BioShop)

0.003% Adenine (Sigma)

The solution was autoclaved and Glucose (Sigma) was added to a final concentration of 2% under a laminar hood.

For solid YPDA, 2% agar was added to the solution before autoclaving.

10X Drop-out medium: The following amino acids were used to prepare the drop-out solution

0.02% L-Adenine

0.02% L-Arginine HCl

0.02% L-Histidine HCl (monohydrate)

0.1% L-Isoleucine

0.03% L-Lysine HCl

0.02% L-Methionine

0.05% L-Phenylalanine

0.2% L-Threonine

0.03% L-Tyrosine

0.02% L-Uracyl

0.15% L-Valine

The solution was autoclaved and stored at 4°C.

Synthetically defined medium: The synthetically defined medium (SD) was prepared

0.67% Yeast nitrogen base without amino acids (Sigma)

1X Drop-out medium

2% Agar (BioShop)

After autoclaving, glucose was added to a final concentration of 2% and the media was poured into sterile petri plates and allowed to solidify in a laminar hood. Plates were later stored at 4°C.

X-αGal: Stock solution for X-αGal was prepared in dimethylformamide (DMF, Fluka) with a concentration of 20mg/ml. The stock was stored at -20°C.

Aureobasidin A: Stock solution of aureobasidin A (CloneTech) was prepared in 96% ethanol with a concentration of 500µg/ml. The solution was stored at 4°C.

For selection: The SD medium prepared above lacks two essential amino acids (Leucine and tryptophan), and is thus named Double drop out (DDO) medium. DDO medium lacking Histidine and Adenine in addition is called quadruple drop out (QDO) medium [QDO = DDO-His-Ade]. QDO further supplemented with X-αGal (40ng/ml) and aureobasidin A (500µl of stock/1000ml of medium) is QDO+. X-αGal and aureobasidin A aid with visual distinction of interaction between investigated proteins. Bluish green colonies on QDO+ confirm positive interaction.

10X TE buffer: 10X TE buffer stock was prepared as follows and stored at -20°C.

100mM Tris-HCl pH 7,5 (Sigma)

10mM

LiAC solution: A 1M stock solution of Lithium Acetate was prepared in milliQ water and stored at RT after filteration with 0.22µm syringe filters (Millipore). The solution was stored at RT.

PEG solution: A 50% solution of Polyethylene glycol 3350 (Sigma) was prepared in milliQ water and filtered using 0.22µm syringe filters (Millipore). The solution was stored at RT.

TE/LiAc buffer: To prepare 1.1X TE/LiAc buffer, a solution with the following final concentrations of reagents was made

11mM Tris-HCl pH 7,5 (Sigma)

1.1M EDTA pH 8,0 (Sigma)

110mM Lithium acetate (Sigma)

PEG/LiAC buffer: To prepare 1X PEG/LiAc buffer, a solution with the following final concentrations of reagents was made

10mM Tris-HCl pH 7,5 (Sigma)

1M EDTA pH 8,0 (Sigma)

100mM Lithium acetate (Sigma)

40% PEG (Sigma)

Carrier DNA: DNA from salmon, sheared and in concentration 10mg/ml (Amersham) was used in the final working concentration of 10µg/ml.

7. Protoplast preparation and transformation

Enzyme mix for releasing protoplasts: The following enzyme mix was prepared to facilitate the release of protoplast from leaves

1.2% Cellulase (Cellulase Onozuka R10 from *Trichoderma viride*; Serva)

0.4% Macerozyme (Macerozym R10 from *Rhizopus sp*.; Serva)

400mM Mannitol (Sigma)

20mM KCl (Sigma)

20mM MES pH 5.7

The enzyme mix was prepared in milliQ water and filtered using 0.22µm syringe filters (Millipore) before use.

W5 Buffer: W5 buffer was prepared in milliQ water and consisted of

154mM NaCl (Sigma)

125mM $CaCl_2$ (Sigma)

5mM KCl (Sigma)

2mM MES pH 5.7

MMg buffer: To make MMG buffer the reagents were mixed in milliQ water in the following final concentrations

400mM Mannitol (Sigma)

15mM $MgCl_2$ (Sigma)

4mM MES pH 5,7

PEG solution: PEG solution consisted of reagents in the following concentrations

40% PEG-4000 (Sigma)

200mM Mannitol (Sigma)

100mM $CaCl_2$ (Sigma)

W1 buffer: W1 buffer was prepared in milliQ water and consisted of

500mM Mannitol (Sigma)

20mM KCl (Sigma)

4 mM MES pH 5,7

8. GUS staining: The following buffer solutions were used for GUS staining

NaPi buffer**:** A 1 M NaPi (pH 7.0) buffer was prepared by using the following buffer solutions

57.7 ml 1 M Na2 HPO4

42.3 ml 1 M NaH2 PO4

X-Gluc solution**:** X-Gluc solution was prepared using the following reagents in given final concentration:

100mM NaPi buffer

5mM K-Ferrocyanide (Sigma)

5mM K-Ferricyanide (Sigma)

100mg X-Gluc (Sigma)

9. Kits

Kit	Use	Manufacturer
GenElute Gel extraction and DNA purification kit	Extraction of DNA fragments from gel; PCR product cleanup	Sigma
GenElute Plasmid miniprep kit	Plasmid isolation and purification from bacteria	Sigma
Direct-zol RNA Mini Prep kit	RNA isolation	Zymo Research
TURBO DNAse free kit	DNAse treatment of RNA	Thermo Fischer
Gateway LR Clonase II enzyme mix	Gateway cloning	Thermo Fischer
2X Power SYBR Green PCR Master Mix	Real time PCR	Applied Biosystems
TaqMan Universall II Master Mix with UNG	miRNA quantification	Applied Biosystems
SENSE Total RNA-Seq Library Prep Kit	sRNA library preparation	Illumina
TrueSeq Small RNA Library Preparation Kit	Library preparation after m^6A-IP	Lexogen
Agilent RNA 6000 Nano Kit	Quantification and quality control of RNA	Agilent Technologies
Agilent High Sensitivity DNA Kit	Quantification and quality control of libraries	Agilent Technologies
Matchmaker Gold Yeast Two Hybrid system	Yeast Two Hybrid	CloneTech
IllustraMicroSpin G-25 Columns	Purification of radiolabeled oligos	GE Healthcare

10. Enzymes

Enzyme	Use	Manufacturer
CloneAmp HiFi Polymerase	Gene amplification	CloneTech
FastDigest restriction enzymes: NdeI, SalI, ClaI, SmaI, PstI, EcoRI, BamH1, NotI, AscI/SgsI	Digestion of insert and vector ends	Thermo Fischer
T4 DNA Ligase	Ligation of vector and insert	Thermo Fischer
SuperScript III Reverse Transcriptase	cDNA preparation	Thermo Fischer
DreamTaq DNA polymerase	Colony PCR	Thermo Fischer

4.2 Methods

4.2.1 Bacterial transformation

E. coli transformation: Chemically competent *E. coli* cells (100 µl) were thawed on ice for approx. 20 minutes. The desired DNA content (ligation mixture, plasmid or LR reaction product) was added to bacterial competent cells and mixed with gently tapping. The mixture was incubated on ice for 30 minutes after which bacterial cells were "heat shocked" by incubation at 42˚C for 1 minuted and immediately afterwards were put on ice for additional 2 minutes. 500 µl of pre-warmed LB liquid medium was added to the transformed bacterial cell suspension. The tube was inverted few times to mix contents properly and the sample was incubated for 1 hour at 37˚C with gentle shaking (350 rpm) on a shaker (Thermomixer Comfort, Eppendorf). Post transformation 150µl of the transformed mixture was then plated on a solid LB media containing appropriate antibiotic for selection of transformants.

A. tumefaciens transformation: Electro-competent *A. tumefaciens* cells (50 ul) were thawed on ice for approx. 20 min. The desired DNA content (ligation mixture, plasmid or LR reaction product) was added to bacterial competent cells and mixed with gently tapping. An electroporation cuvette (Bio-Rad, USA) was pre-chilled on ice and competent cells were transferred into the cuvette and kept on ice. The cuvette was swiftly put in the ShockPod cuvette chamber of Gene Pulser Xcell system (Bio-Rad) and a pulse of 2.5 kV (129ohm resistance) was applied, and 1 ml of a liquid LB medium was immediately afterwards. After gently mixing the bacteria the solution was transferred to a micro-centrifuge tube and incubated at 28°C for 1 hour with gentle shaking. Post transformation 150µl of the transformed mixture was then plated on a solid LB media containing appropriate antibiotic for selection of transformants.

4.2.2 RNA isolation and cDNA preparation

RNA was isolated from 4 weeks old leaves using Direct-zol™ RNA kit (Zymo Research). 100mg of ground material was used per isolation. Isolated RNA was quantified using DS-11 Denovix spectrophotometer (Denovix, Wilmington, Delaware, USA) and additionally, agarose gel electrophoresis was done to test the quality of RNA as well. For DNAse treatment RNA was treated with TURBO DNAse (TURBO DNA-free kit, Thermo Fisher) and quality and quantity of RNA was tested again using above described methods.

For regular cDNA preparation 3µg of RNA was used for first strand synthesis using Oligo (dT) primers and SuperScript III Reverse Transcriptase (Thermo Fisher) according to manufacturer's protocol. The reverse transcription was carried out by incubating the samples at 50°C for 1 hour followed by 60°C for 15 min.

For cDNA preparations to be used for TaqMan assays, cDNA was synthesised from 10 ng of the total DNase-treated RNA using a miRNA-specific reverse transcriptase primer (custom produced by Thermo Fisher) and MultiScribe Reverse Transcriptase (Thermo Fisher), according to the manufacturer's protocol. Reverse transcription reaction followed the following thermal profile.

Temperature	Duration
16°C	30 min
42°C	30 sec
85°C	5 min

4.2.3 PCR

Regular PCRs for amplification of target genes were performed using CloneAmp HiFi PCR Premix (CloneTech). A 25µl reaction was prepared with 1X concentration of CloneAmp HiFI PCR premix, 0.3µM of Forward and Reverse primers and ~100ng of template. The following PCR program was run on a Veriti^{TM} Thermal Cycler or ProFlex PCR system (Applied Biosystems).

Temperature	Duration	
98°C	1 min	
98°C	10 sec	30-35 cycles
55°C	15 sec	
72°C	30–60sec/kb	
72°C	5 min	

PCRs for identification of positive colonies post transformation of bacteria were performed using DreamTaq polymerase (Thermo Fisher). A 10µl reaction/sample was prepared with final concentrations as follows: DreamTaq buffer (1X), dNTP mix (0.2mM), Forward and Reverse

primers (0.5µM) and DreamTaq polymerase (0.05U/µl). One colony was picked with a tip and mixed in the 10µl PCR mix contained in a PCR tube. PCR was run according to the following program.

Temperature	Duration	
95°C	10 min	
95°C	30 sec	25 cycles
59°C	30 sec	
72°C	1 min	
72°C	15 in	

4.2.4 Quantitative Real time PCR

For estimation of pri-miRNA levels SYBR Green PCR MasterMix (Applied Biosystems) was used to prepare PCR reaction which contained 5µl of 2X Power SYBR Green PCR MasterMix, cDNA, and gene-specific primers (200nM each) in a final volume of 10µl. PCR reactions were run either on 7900HT Fast Real-Time PCR System (Thermo Fisher) or Quant Studio & Flex Real-Time PCR system (Thermo Fisher) in minimum three biological replicates. All of the results were analysed using Microsoft Excel and SDS 2.4 software (Thermo Fisher). The statistical significance of the results presented was estimated using a Student's t-test at three significance levels: *$p < 0.05$, **$p < 0.01$, and ***$p < 0.001$.

For miRNA quantification TaqMan Universal Master Mix (Applied Biosystems) was used and reactions were performed according to manufacturer's instructions. The following PCR profile was used for RT-qPCR with SYBR Green master mix.

Temperature	Duration	
95°C	10 min	
95°C	15 sec	40 cycles
60°C	1 min	
95°C	15 sec	Melting curve
60°C	15 sec	
95°C	15 sec	

For TaqMan PCRs similar profile as presented above was used with the exclusion of the melting curve stage.

4.2.5 Agarose gel electrophoresis

For PCR products: 3-5µl of PCR products were mixed with 2X HSE or 6X Orange loading buffers and loaded on to 1% agarose gel containing EtBr. Electrophoresis was run using 1X TBE in Hoefer HE33 Mini Submarine System (Hoefer INC, Holliston, USA) at 60-65mA. The products were visualized using Gene Box (Syngene) with the Gene Snap software.

For RNA: 1µl of RNA was mixed with 2X RNA loading buffer and denatured at 95°C for 2 min. Samples were kept on ice for 1-2 min immediately after denaturation. Denatured samples were loaded on 2% agarose gel and electrophoresis was carried out as mentioned above. Results were visualised using same equipment as above.

4.2.6 m^6A Immunoprecipitation

RNA was isolated from 4 weeks old leaves of WT, *mta* and *tgh* plants. Upto 500 mg of RNA was used to purify polyA RNA using NucleoTrap mRNA isolation kit (Macherey-Nagel). 10µl of polyA RNA (1µg/µl) was used for immunoprecipitation. Immunoprecipitation was performed using EpiMark N6-Methyladenosine Enrichment Kit (NEB). Briefly, 25µl (per sample) of magnetic Dynabeads protein G (Thermo Fisher) were washed with 250µl of IP buffer and 2µl of anti- m^6A antibody/per sample (from the kit) was incubated with the beads for 1 hour at 4°C/2rpm. Beads were washed with IP buffer again and resuspended in 250µl of IP buffer. 3µl of RNAse Inhibitor (Promega) was added to the beads. 10µg of polyA enriched RNA was spiked in with 1µl of positive and negative controls (from the kit; diluted to 1:1000) to make the final volume to 12µl. 10% (1.2µl) was aliquoted to be used as the input and the rest was added to the beads. The reaction mixture was incubated for 2 hours at 4°C/2rpm. Post incubation, beads were washed twice with IP buffer (first:1ml; second: 200µl). Next, the beads were washed with 200µl of HSB containing 0.075% NP-40 followed by another wash with HSB but without NP-40. Finally, two washes with 200µl of LSB complete the washing steps.

Beads were resuspended in 40µl of IP buffer and 4µl of Proteinase K and 0.4µl of 10% SDS were added to the mix. The samples were then incubated for 1 hour at 50°C. After incubation, 40µl of Acid Phenol:Chloroform (pH:4.5) was added to the samples and they were

vortexed for 20 seconds followed by centrifugation at 14,000 rpm for 5 min. at RT. The top aqueous layer was taken and 40µl of chloroform was added followed by vortexing and centrifugation at 14,000 rpm for 5 min. at RT. The aqueous layer was taken and ethanol was added (5x by volume) along with sodium acetate (10% volume of aqueous layer) and GlycoBlue co-precipitant (Thermo Fisher). The samples were left overnight at -20°C for precipitation. Next day samples were centrifuged at 14,000 rpm for 30 min/4°C. The RNA pellet was then washed with pre-chilled 75% ethanol and dissolved in 11µl of RNAse free water. RNA was then used either for library preparations or cDNA synthesis for RT-qPCR. The procedure is presented as a schematic below (Figure M1).

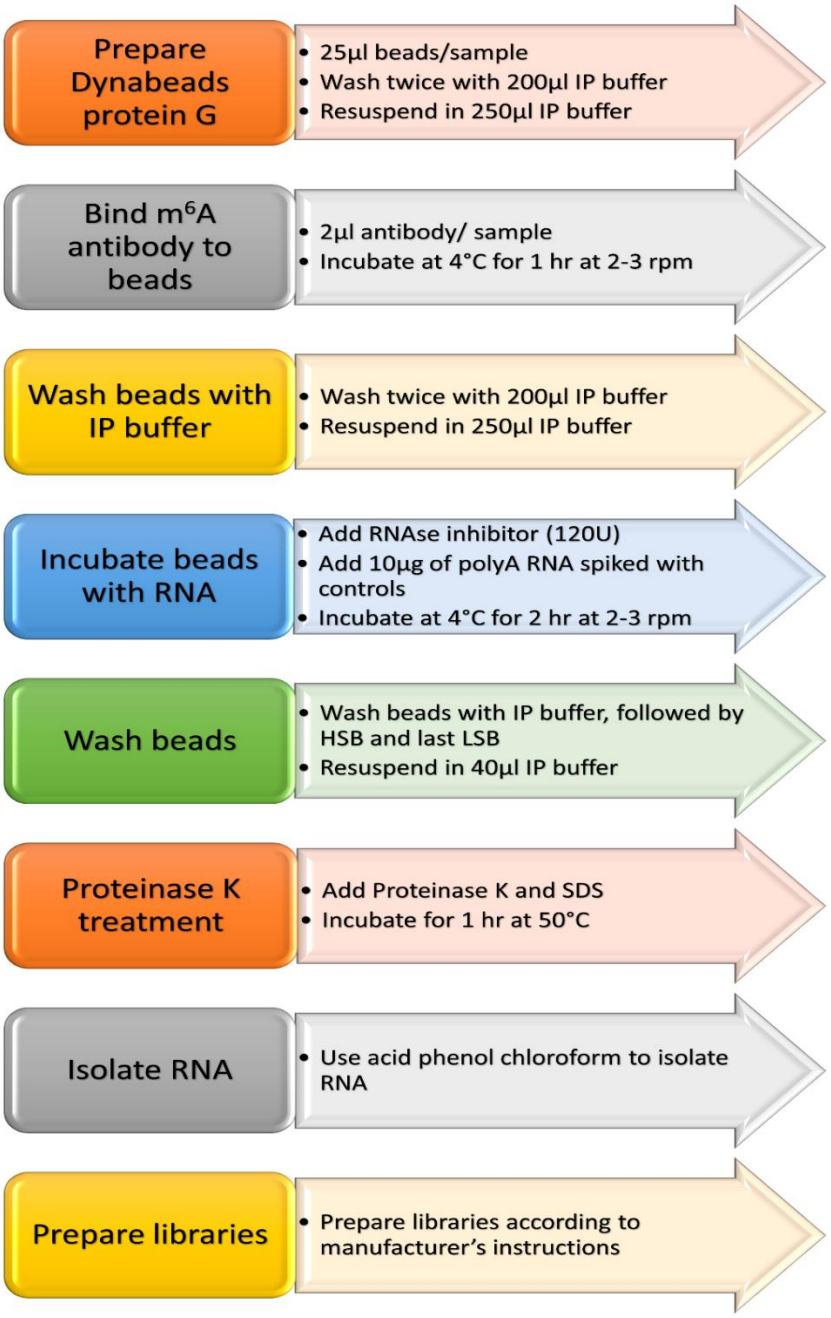

Figure M1 Immunoprecipitation of m^{6}A methylated RNA. A schematic representation of the steps involved in identifying RNA transcripts that are m^{6}A methylated is outlined.

4.2.7 RNA immunoprecipitation

4 weeks old leaves from WT, *mta* mutants and transgenic *Arabidopsis* line containing *p35S:MTA-GFP* and GFP alone were crosslinked using 1% formaldehyde and vacuum infiltrating for 10 min and next quenched with 125mM glycine and frozen in liquid nitrogen. 3-

4g of ground tissue was used for further experiments. For isolation of nuclei the ground tissue was dissolved in 40ml of ice-cold nuclei isolation buffer I by vigorous vortexing and filtered through Miracloth in a 50ml tube. The Miracloth was then washed with 10ml of buffer I in the same tube. The solution was centrifuges at 4000g/4°C for 20min. The supernatant was discarded and the pellet was resuspended in 1ml of ice-cold nuclei isolation buffer II. The solution was transferred to a 2ml microcentrifuge tube and centrifuged at 10,000rpm/4°C for 10 min. The step was repeated until a white pellet was obtained (usually 3-4 times). After a white pellet was obtained, the pellet was dissolved in 300µl of buffer II. 1.5ml microcentrifuge tubes (1/sample) were prepared with 900µl of ice-cold nuclei isolation buffer III. The 300µl buffer II solution, containing the dissolved pellet, was gently pipetted on top of buffer III. The tubes were centrifuged at 16,000g/4°C for 30 min. The supernatant was discarded and the pellet was dissolved in 300µl of sonication buffer. These are the isolated nuclei.

Post isolation, nuclei were sonicated at 4°C using Bioruptor® (Diagenode) at high intensity for 2 cycles (30 sec ON/30 sec OFF). The water bath was kept at 4°C during sonication. The samples were then centrifuged at 10,000rpm/4°C for 5min. The supernatant was taken in a fresh 2ml tube and diluted 3X times by adding 600µl of IP buffer. 10% of the sample was aliquoted and saved as Input sample. Rest of the sample was used for immunoprecipitation. GFP-Trap®_MA (Chromotek) magnetic beads and native HYL1 antibodies (Agrisera) bound to DynaBeads Protein G (Invitrogen) were used to immunoprecipitate RNA fractions bound by MTA or HYL1. RNA was isolated from input (control) and IP samples and treated with TURBO DNAse followed with cDNA preparation as described in 4.2.2. Real time was performed as described in 4.2.4. Experiments were done in 3 biological replicates and statistical significance was calculated using student's T-test. A schematic of the procedure is presented below (Figure M2).

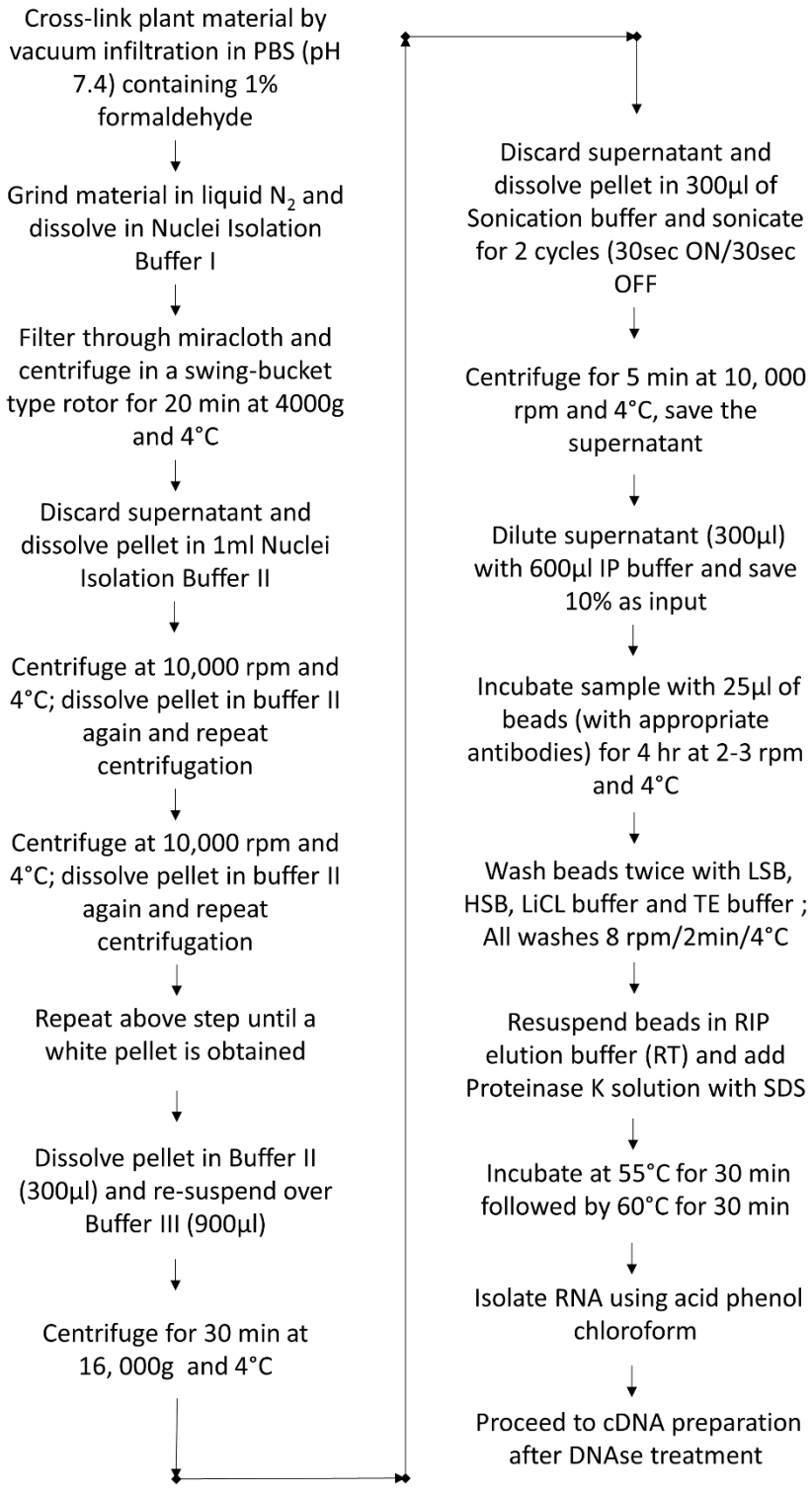

Figure M2 RNA Immunoprecipitation protocol. A step by step scheme of RNA immunoprecipitation using cross linked plant material is presented. All steps should be carried out at 4°C unless other specific temperatures are specified.

4.2.8 Library preparation and sequence analysis

For small RNAs: Libraries were prepared from the obtained sRNA fraction of WT and *mta* plants using TrueSeq Small RNA Library preparation Kit (Illumina) according to manufacturer's instructions. Libraries thus obtained were quantified on Agilent Bioanalyzer 2100 system and sent to Fasteris, Geneva, Switzerland for sequencing on the HiSeq 4000 platform. The obtained raw sequences were cleaned off the adapter sequence using FASTX-Toolkit and the clean reads were mapped to all mature *A. thaliana* miRNAs from miRBase (release 22) using script: countreads_mirna.pl. Sequencing was done in 3 biological replicates and R-package NOISeq was used to normalize the reads and to calculate fold change and false-discovery rate (FDR).

For m^6A-IP samples: RNA obtained after immunoprecipitation (IP samples) and RNA from Input samples (used as control) was used to prepare libraries using the SENSE Total RNA-Seq Library Prep Kit (Lexogen). Libraries thus obtained were quantified using the Agilent Bioanalyzer 2100 system and were sequenced at Fasteris, Geneva, Switzerland on the HiSeq 4000 platform. FASTX-Toolkit was used to trim the first 30 nucleotides of the raw reads obtained and adapters were removed using Trimmomatic while rRNA sequences where removed with Bowtie. *Arabidopsis* TAIR10 was used as the reference genome to align the clean reads using HISAT2 (the overall alignment rate was 89-92% for each sample). Salmon was used to estimate transcript-level abundance for RNA in clean reads. Known pri-miRNA transcripts described in the mirEX[2] database and sequences of the spiked in m^6A controls were supplemented to the multifasta file with *A. thaliana* reference transcripts (cDNA and ncRNA) for quasi-mapping. The spiked-in unmodified RNA control was used to normalize the TPM values. TPM values in input and IP samples where normalized with the use of unmodified RNA spike-in control. Enrichment was calculated using TPM value with the following formula: (wt IP/input) / (mta IP/input).

4.2.9 Yeast Two Hybrid

Matchmaker Gold Yeast Two Hybrid System (CloneTech) was used to perform the Yeast two Hybrid experiments. CDS of MTA along with its known interacting partners (MTB and FIP37) and potential interactors (miRNA biogenesis related proteins: SE, HYL1, CDF2, TGH,

CBP20 and DDL1) were cloned into a vector containing either the activation or binding domain (AD or BD). A single colony of *S. cerevisiae* strain Y2HGold was grown in 1X YPDA medium overnight at 28°C with 180-250 rpm shaking. The overnight grown culture was sub cultured until optical density of 0.6 was reached. The culture was centrifuged at 700g for 5 min to sediment the yeast. After washing sterile water, yeast was suspended in 1.1X TE/LiAC buffer and centrifuged for 15 sec at high speed. The sedimented yeast was dissolved in 600µl of 1X Ti/LiAC buffer. A microcentrifuge tube (1.5 ml) was used to mix competent yeast cells (prepared above) with 700ng of plasmids [with a combination of AD and BD vectors (containing protein of interest or empty vectors as controls)] and carrier DNA. A PEG/LiAC solution was added to the tube and incubated for 30 min at 30°C with 1000rpm shaking. Afterwards, DMSO was added to the tube, mixed and incubated at 42°C for 20 min. Cells were pelleted at high speed for 15sec and resuspended in 1X TE.

Transformed yeast cells were plated on SD medium lacking Leucine and Tryptophan (DDO) for selection of transformed yeast. Yeast was also plated on DDO medium lacking Adenosine and Histidine (QDO) and QDO medium supplemented with X-αGal and Aureobasidin A (QDO+). QDO and QDO+ medium was used to identify positive interactions between target proteins.

4.2.10 Confocal Microscopy

CDS of MTA along with its known interacting partners (MTB and FIP37) and potential interactors (miRNA biogenesis related proteins: SE, HYL1, CDF2, TGH, CBP20 and DDL1) were cloned into pSU3 and/or pSU5 vectors (with GFP/RFP tag) via Gateway cloning. Protoplasts were isolated from leaves of 3-4 weeks old WT *Arabidopsis* plants using Tape-Arabidopsis Sandwich method[118]. Leaves with the lower epidermal layer removed were kept in a petri-dish and immersed in an enzyme mix containing cellulase (1% w/v) and macerozyme R- 10 (0.2% w/v). Leaves were incubated with the enzyme mix for 45 min at RT (20-25 rpm shaking) in dark. The protoplast thus released were then centrifuged in a swinging bucket rotor at 160-180g for 5 min followed by two washes with W5 buffer. Protoplasts were then dissolved in 1 ml of MMg solution.

2ml microcentrifuge tubes were pre-prepared with 5µg of desired plasmid(s) and 100µl of prepared protoplast solution was added to the tubes using tips with chopped ends. 100µl of PEG-4000 solution was added to the tube and was gently mixed by tapping. After incubation

for 5 min, 450µl of W5 solution was added to the tube and mixed by tapping followed by centrifugation at 300g for 3 min. Pelleted protoplasts were resuspended in 300µl of W1 solution. After 7-10 hours of incubation, protoplasts were observed under a confocal microscope (Nikon A1Rsi), and FRET-FLIM measurements were undertaken using the PicoHarp300-Dual Channel SPAD system (PicoQuant). SymPhoTime 64 software was used to calculate fluorescence lifetimes of GFP labelled proteins. 9 cells were analyzed for each sample and statistical significance was calculated using the Student's t-test.

4.2.11 Co-Immunoprecipitation

Co-immunoprecipitation was done following the steps of RNA immunoprecipitation (4.1.12) with few changes. The sonication of nuclei was done for 10 cycles (30sec ON/30sec OFF). The samples were centrifuged after sonication and were incubated with GFP trap agarose beads (Chromotek). After the respective washing steps the beads were dissolved in 200µl of TE buffer. The solution was sent to Institute of Biochemistry and Biophysics, Polish Academy of Sciences, Warsaw.

For the mass spectrometry analysis, beads bound with our target proteins (MTA-GFP and GFP) were pelleted and re-suspended in ammonium bicarbonate buffer (100mM) and treated with DTT (100mM) for 30 min at 57 °C. This was followed by treatment with iodoacetamide (50mM) for 45 min at RT in the dark. The proteins were then digested overnight at 37°C using 100 ng/µl trypsin (Promega). Nano-Ultra Performance Liquid Chromatography was used to fractionate peptide mixtures which were then run on Orbitrap Velos mass spectrometer (Thermo). Peptides were identified with Mascot algorithm (Matrix Science, London, UK) and searched against the TAIR10 database. Each protein was quantified by the total number of MS/MS fragmentation spectra in two replicates. Statistical analysis was done using the R program.

4.2.12 Northern hybridization

RNA was isolated from leaves of *Nicotiana benthamiana* that were transfected with the desired construct(s) after 72h of transfection. 30µg of RNA per sample was denatured at 95°C for 2 min and then separated on 15% poly acrylamide gel supplemented with 8M urea. Electrophoresis was carried out at 300V for around 4-5h or until the bromophenol dye reached

the bottom of the gel. After electrophoresis, RNA was transferred to Amersham Hybond NX membrane soaked in 0.5X TBE. Two pieces of blotting paper were soaked in 0.5X TBE and stacked on top of each other followed by the membrane. Gel was put on top of the membrane and a glass rod was used to gently level the stack and remove any air bubbles. Two more pieces of blotting paper were stacked on the top of the gel. Transfer was done for an hour at 10V using Trans-Blot Electrophoretic Transfer Cell (Bio-Rad). After transfer, RNA was cross linked to the membrane by applying 120 kJ/cm2 of UV light (using CL-1000 Ultraviolet Crosslinker (UVP)) on the RNA side of the membrane, twice.

DNA probes, perfectly complementary to the target RNA were radiolabelled by preparing the following mixture: 2µl of 10µM probe; 5µl of γ32P-ATP (6000 Ci/mmol); 2µl of T4 polynucleotide kinase buffer;1µl of T4 polynucleotide kinase 10U/µl (Roche) and DEPC treated water to a final volume of 20µl. The reaction mix was incubated at 37°C for 45 min and un-incorporated γ32P-ATP was removed by spinning the mixture in Illustra MicroSpin G-25 column.

For hybridization, membrane crosslinked with RNA was placed RNA side up in a hybridization glass bottle and treated with 5ml of pre-warmed hybridization buffer (42°C) for 30 min at 42°C with rotation. Post incubation, the hybridization buffer was exchanged for fresh 5ml of hybridization buffer and the radiolabelled oligo mixture was added to the bottle. Bottle was incubated at 42°C with rotation overnight. Next, the membrane was washed with 2x SSC buffer for 15 min (repeated twice). Hybridization signals were visualized using FLA5100 (Fuji) and results were analysed using Multi Gauge v2.2 software.

4.2.13 GUS staining

For GUS staining *mta* plants carrying a *proDR5:GUS* gene was used along with WT as control. 2 weeks old seedlings grown in ½ MS medium were kept in the X-Gluc solution at 37°C for 24h. Seedlings were then washed with 70% ethanol for two days and then mounted in 50% glycerol (v/v). The leaves were then observed under Leica M60 microscope.

5 Results

5.1 Lack of m^{6}A methylation causes defects in miRNA biogenesis

m^{6}A is an essential epigenetic modification and the complete knockdown of any core member of the methyl transferase complex: MTA/FIP37/MTB, results in embryo lethality[92,94]. Hence, we worked with plants that have a very low expression of MTA in adult plants. These plants were obtained from Dr. Rupert Fray's lab (University of Nottingham). *mta* hypomorphic mutant carries MTA cDNA under the *ABI3* promoter, in the background of homozygous SALK_074969 line[119]. *ABI3* promoter drives the gene expression enough to rescue embryo lethality but in adult plants m^{6}A methylation levels are 90-93% lower than WT plants[119]. These plants can be visualised in the figure below (Fig 1). The *mta* hypomorphs are much smaller than the WT plants with crinkled leaves, and a bushier and shorter inflorescence. However, they produce flowers and viable seeds.

Figure 1 Wild type Col-0 (WT Col-0) plants are visualised next to *mta* hypomorphic mutant. *mta* mutants are much smaller in size as compared to WT plants with more crinkled leaves. Scale bar = 1cm on top right.

Our first goal was to test whether we could observe any changes in miRNA levels in *mta* plants as compared to WT plants. Our sRNA sequencing data showed us an overall decrease in the miRNA levels in *mta* plants (Fig 2a). 60 miRNA species were identified with high confidence scores (probability > 0.9) and false discovery rate of 0.1 providing statistical significance to this data. Out of these 60, 51 miRNA species were down regulated while only 9 were upregulated (Fig 2b). An orthogonal approach of TaqMan RT-qPCR was used to confirm this downregulation for 6 randomly selected miRNAs, namely miR159b, miR169a, miR319b, miR396b, and mir399a and miR850 (Fig 2c).

We then tested the pri-miRNA levels in *mta* hypomorphic plants. Our RT-qPCR experiment was based on the mirEX^2 platform developed in our lab[120,121]. A total of 298 pri-miRNAs were tested for this experiment out of which 68 could not be detected using RT-qPCR. 230 pri-miRNAs were analysed for their expression levels and out of these 85 were found to have statistically significant differential expression in *mta* hypomorphic plants. 56 out of 85 pri-miRNAs (~ 66%) were upregulated while 29 were downregulated, as shown in the volcano plot (Fig 2d). We also found 20 miRNA/pri-miRNA pairs which had accumulated levels of pri-miRNAs and lower levels of mature miRNAs (Fig 2e). These data conclusively show that in the lack of m^{6}A methylation the process of miRNA biogenesis is in-efficient. The outliers to our data: the 9 upregulated miRNAs and 29 down regulated pri-miRNAs could be observed because of indirect effects caused by m^{6}A modification which are discussed further in the Discussion chapter.

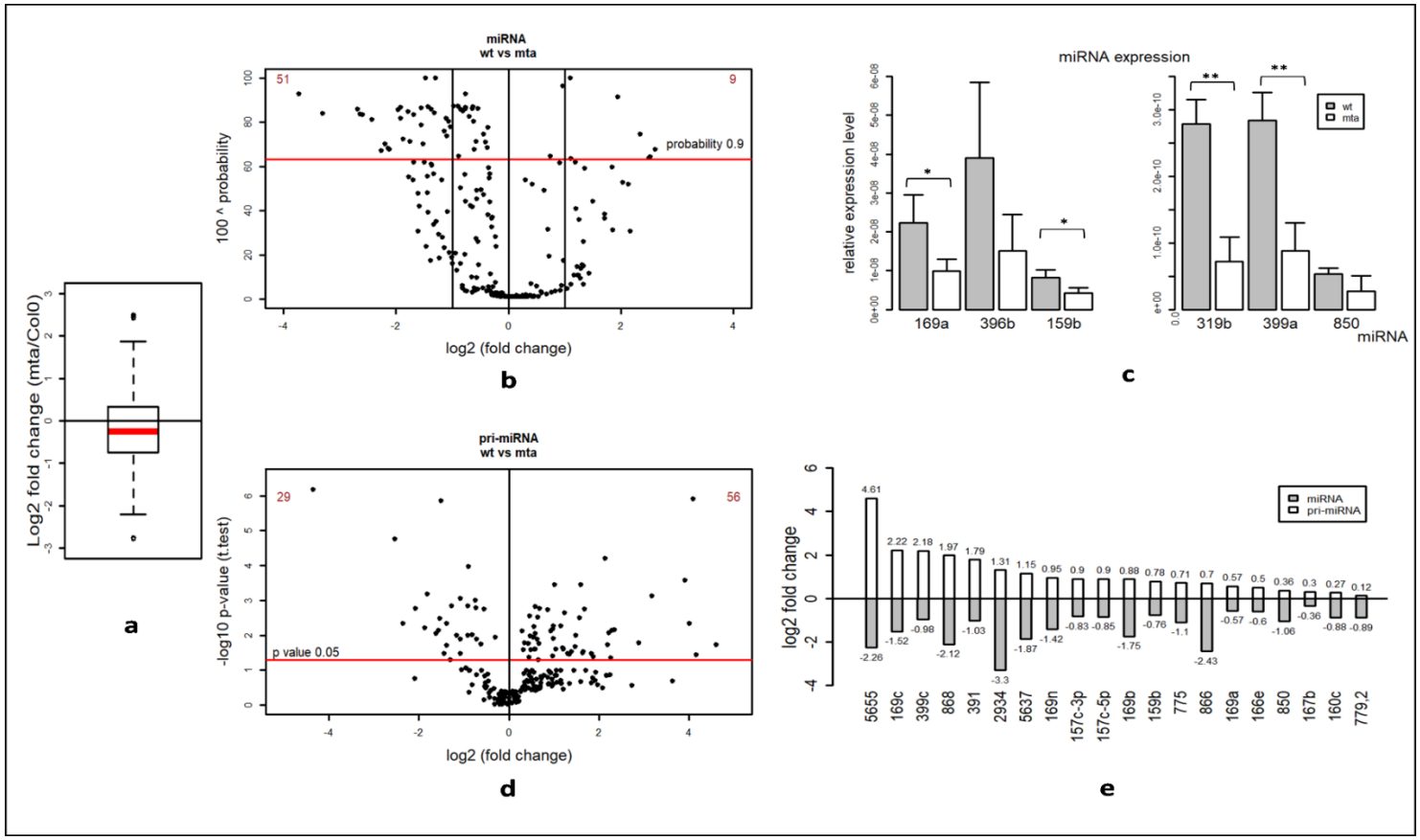

Figure 2. miRNA biogenesis is hampered in *mta* hypomorphic plants. (a) An overall decrease in miRNA levels represented by a box plot. Red line represents median value. **(b)** Expression level of mature miRNA in *mta* hypomorphs vs WT plants. One black dot represents one miRNA. Red line represents the probability threshold of 0.9. **(c)** Relative expression levels of 6 miRNAs as observed using TaqMan RT-qPCR. These examples were randomly selected from miRNAs identified above the threshold in pane (b). * = p-value < 0.05, ** = p-value < 0.005 and error bars represent standard deviation (n=3). **(d)** Differential expression levels of 230 pri-miRNAs in *mta* plants vs WT are represented in a volcano plot. Each black dot represents one pri-miRNA. Red line is the threshold of statistical significance with p value 0.05. **(e)** 20 cognate pairs of miRNAs (downregulated) with their corresponding pri-miRNAs (upregulated) are presented. These were selected from the data presented in panel b and d.

5.2 Pri-miRNAs carry m^{6}A mark deposited by MTA

Having established that lack of m^{6}A is indeed detrimental to miRNA biogenesis in *Arabidopsis*, we then asked whether we could identify a direct interaction between MTA and pri-miRNAs. We also tested whether we could detect m^{6}A methylation in pri-miRNAs. To investigate m^{6}A methylation status of pri-miRNAs we used m^{6}A-IP followed by next generation sequencing (NGS). PolyA RNA fraction was used for this experiment to get rid of the unnecessary signals of ribosomal and other non-coding RNAs. Our protocol did not use RNA fragmentation to avoid any loss of pri-miRNA signals. A positive control RNA (with m^{6}A modification) and one negative control (no m^{6}A modification) were spiked in the RNA sample before the IP. The robustness of the method was tested by monitoring the enrichment of spiked in RNA controls (Fig 3a). The sequencing data was filtered to consider only those *MIR* genes transcripts that are derived from independent transcriptional units excluding the ones that are located in the introns of protein coding genes. Our analysis identified 11 *MIR* gene transcripts that were enriched >1.5 fold in WT plants as compared to *mta* hypomorphic mutant. In this case an enrichment in WT samples meant that these pri-miRNAs are m^{6}A methylated in WT plants but not in our mutant, as expected. These data can be seen in Fig 3b and c.

A direct association of MTA with pri-miRNA was analysed using RNA immunoprecipitation (RIP) followed by RT-qPCR. Crosslinked plant material from *35S:MTA::GFP* transgenic line was used to isolate the nuclei and RNA fraction bound by MTA was precipitated using anti-GFP antibody. Using this approach, we tested 10 pri-miRNAs identified in our m^{6}A-IP sequencing data. We found that 8 out of these 10 pri-miRNAs were significantly enriched in MTA-GFP sample as compared to control GFP sample (Fig 3d). These data combined with our m^{6}A-IP seq data clearly show that MTA binds to pri-miRNAs and methylates them.

m^{6}A methylation is present within a specific RRACH motif, as mentioned in the introduction. We wanted to know whether the pri-miRNAs identified in these data also carry such a motif. GGAC and AGAC are the most common motifs observed in plant systems[93]. We looked for these two motifs in our 11 pri miRNAs and found that 10 out of the 11 indeed had GGAC or AGAC motif within the pri-miRNA sequence. Interestingly, for 6 examples (pri-mir163, pri-mir166a, pri-mir824, pri-mir830, pri-mir850 and pri-mir5642a) the motif was present within the stem-loop region of pri-miRNAs. These observations are summarized in tabular format in Fig 3e.

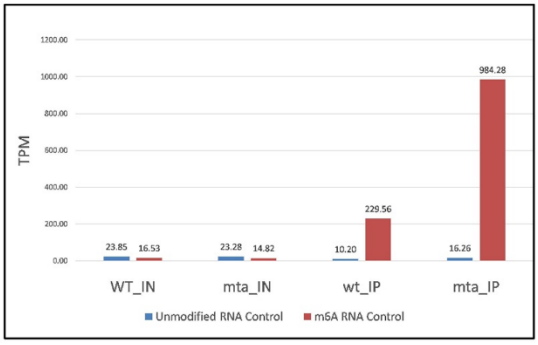

a

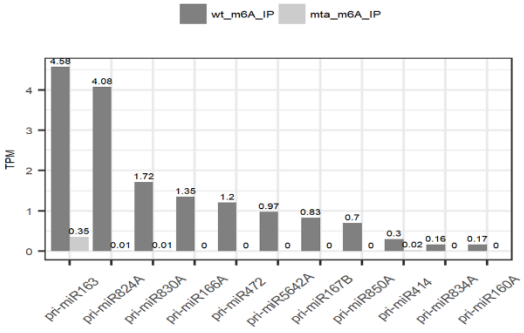

b

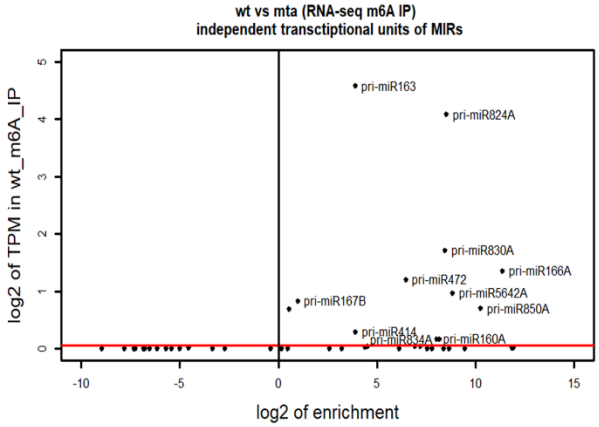

c

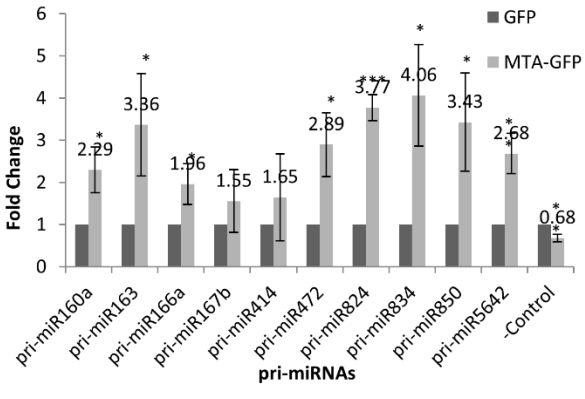

d

pri-miRNA	Motif	Location wrt to pre-miRNA
160a	GGAC	123bp upstream
163	GGAC	Within the miRNA
166a	GGAC	Within the miRNA
167b	GGAC	6bp downstream
414	AGAC	22bp upstream
472	AGAC	78bp downstream
824	AGAC	Within the miRNA
830	AGAC	Within the pre-miRNA
834		None detected
850	GGAC	Within the miRNA
5642a	AGAC	Within the pre-miRNA

e

Figure 3 MTA binds to pri-miRNAs and methylates them. (a) Enrichment of m^6A modified RNA control (red colour) that was spiked in the samples can be seen in m^6A immunoprecipitated samples (WT_IP and *mta*_IP) but not in the input samples (WT_IN and *mta*_IN). No enrichment of unmodified RNA control (blue colour) was observed. **(b)** Transcripts from *MIR* genes that were found to be enriched in WT samples after immunoprecipitation (WT_m^6A_IP) but not in *mta* samples (mta_m^6A_IP). **(c)** A volcano plot shows the distribution of *MIR* gene transcripts enriched (in $\log_2$ enrichment) in wild type plants as compared to *mta* after m^6A-IP (wt_m^6a_IP). Each black dot represents one transcript. Red line represents the transcript per million (TPM) threshold of 0.05. **(d)** Enrichment of pri-miRNAs in MTA-GFP samples vs control (GFP) samples is presented as fold change. * = p-value < 0.05, ** = p-value < 0.005, *** = p-value < 0.001. **(e)** A table shows the presence of GGAC or AGAC motif within the pri-miRNAs that are m^6A methylated by MTA. Location is presented relative to the pre-miRNA stem-loop that contains miRNA/miRNA*. Upstream is before the pre-miRNA and downstream after.

5.3 HYL1 binding to pri-miRNAs is affected in *mta* hypomorphic plants

The presence of m^6A causes alterations in the secondary structures of RNAs, a phenomenon called 'm^6A switch'[117,122,123]. These absence or presence of these m^6A influenced structural features either allow or prevent the binding of RNA binding proteins to their substrates. Driven by the possibility of m^6A switch affecting DCL1 cleavage, we collaborated with Brian Gregory's lab (University of Pennsylvania, USA) for their expertise in probing secondary structure of RNA using Protein Interaction Profiling sequencing (PIP-Seq). PIP-Seq uses a combination of double strand and single strand specific RNAses to digest RNA. After sequencing the structure of RNA can be predicted by comparing the coverage of each sample[124,125]. Indeed, their structural probing analysis revealed that pri-miRNAs lose secondary structures especially in the stem-loop region in *mta* background (Fig 4a and 4b). We also used a folding algorithm constrained to the structural scores of pri-miRNAs to visualize these structural changes better. These 2D secondary structure distortions can be seen in Figure 5. This observation is crucial as the loss of secondary structure can lead to inefficient binding of Microprocessor complex to the pri-miRNAs. Indeed, my HYL1:RIP-qPCR data shows that

HYL1 can not bind the pri-miRNAs in *mta* background as efficiently as compared to WT background (Fig 4c). HYL1 is a double stranded binding protein and a core member of the Microprocessor complex. Binding of HYL1 to pri-miRNAs is essential for efficient DCL1 activity and the impaired binding of HYL1 to now improperly folded pri-miRNAs is one of the reasons why pri-miRNAs can't be efficiently processed in absence of m^6A.

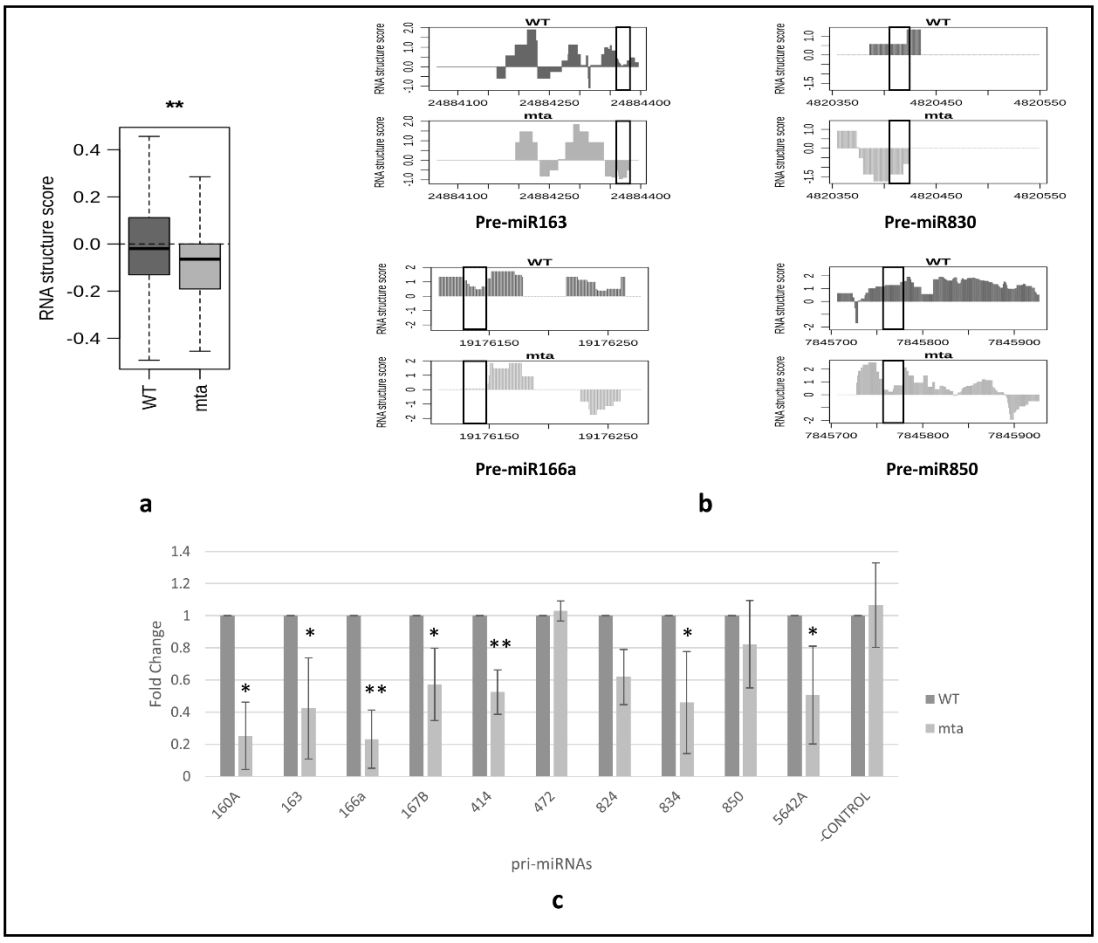

Figure 4 Structural probing anlaysis and the binding of HYL1 to pri-miRNAs. (a) An overall decrease in the prevalence of secondary structures within stem-loop regions of all pri-miRNAs in *mta* mutant can be seen in a box plot. **(b)** A few examples (m^6A methylated) showing clear changes in the structural profiles of pri-miRNAs. Boxes mark the region coding the respective miRNAs. The experiments and analysis were done in the lab of Dr. Brian Gregory. **(c)** HYL1 GFP based immunoprecipitation followed by RT-qPCR shows a decrease in the binding of HYL1 to pri-miRNAs in *mta* background. The examples presented are the same that were identified as m^6A methylated and are bound by MTA as well. Error bars represent standard deviation of 3 biological replicates. * = p-value < 0.05, ** = p-value < 0.005, *** = p-value < 0.001. – Control = *WUSCHEL (WUS)* gene (AT2G17950).

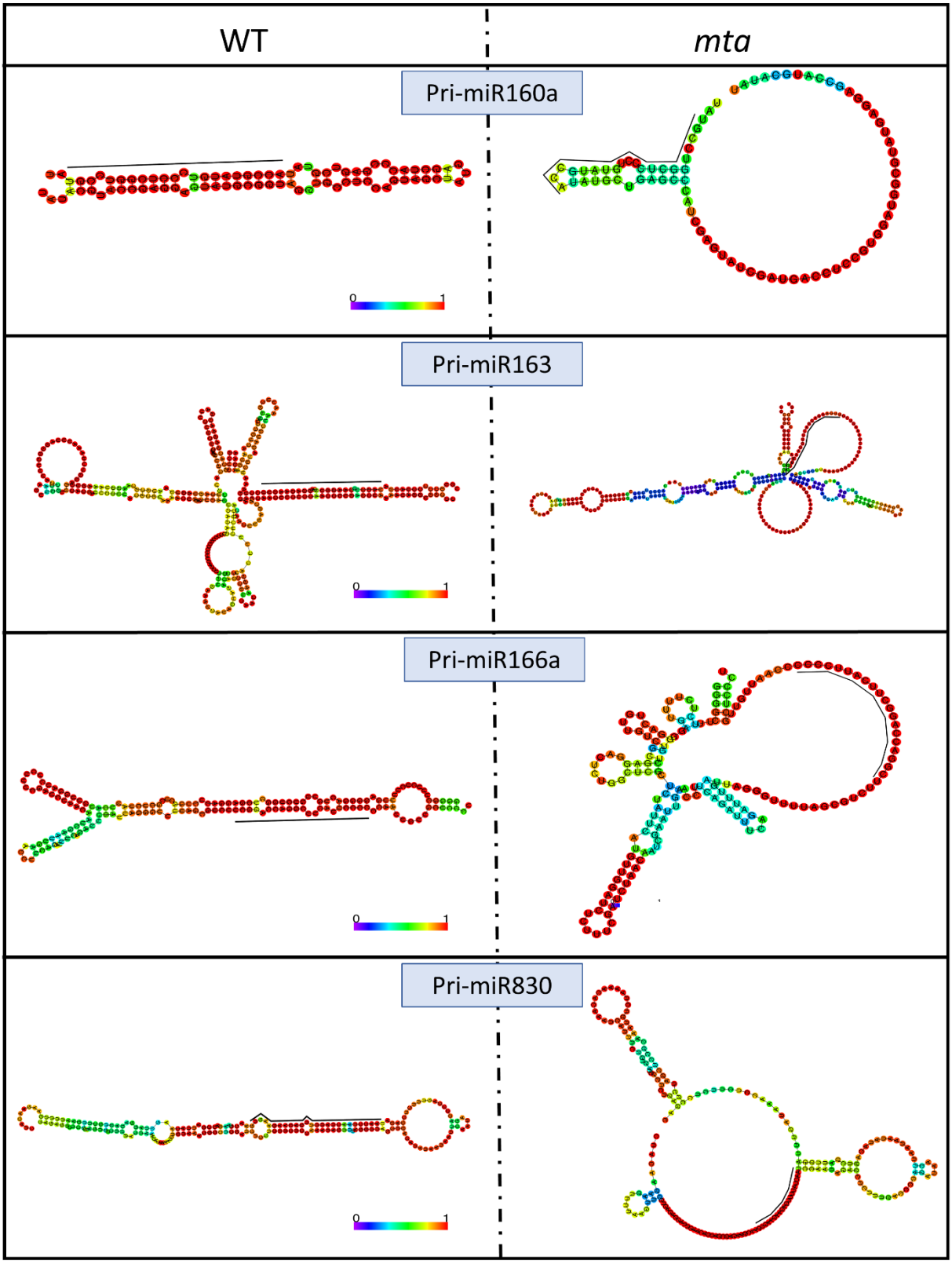

Figure 5 2D structural changes caused by lack of m6A methylation. 2D structures produced by folding constrained to their respective structural scores show the distortion of

canonical stem-loop structures in *mta* mutants (right column). All examples presented have been identified by us as m6A methylated in WT plants. Colour bar presents the probability score of the base pairing as predicted by the algorithm. Red colour: base has the highest probability of being in the single or base paired state as predicted by the algorithm. Other colours present probabilities according to the bar. Analysis was performed in co-operation with Dr Brian Gregory laboratory by Xiang Yu.

5.4 MTA interacts with TGH (a player in miRNA biogenesis) and acts at early stage of miRNA biogenesis

Having established that MTA can directly affect miRNA biogenesis via binding and methylating pri-miRNAs, we then asked if MTA could also affect miRNA biogenesis by interacting with other proteins involved in miRNA biogenesis. We started by performing a yeast two hybrid-based screen of proteins known to be involved in miRNA biogenesis (HYL1, CBP20, CBP80, SE, TGH, NOT2b and DDL1). In our screen we identified TGH and Not2b as a positive interactor with MTA (Fig 6). Unfortunately, we also observed auto activation of TGH in the yeast system meaning that our observation could be false positive.

		HYL1 (BD)	CBP-20 (BD)	CBP-80 (BD)	SE (BD)	TGH (BD)	NOT2 B (BD)	DDL1 (BD)	Control (BD)	TGH (BD)+ Empty
MTA (AD)	DDO									
	QDO									
	QDO+									
Interaction		Negative	Negative	Negative	Negative	Positive	Positive	Negative	Negative	Positive

Figure 6 Yeast two hybrid screen to identify MTA interactors. MTA with activation domain (AD) was tested with other candidate proteins HYL1, CBP20, CBP80, SE, TGH and DDL1 in binding domain (BD). Positive interactions were identified by bluish green colonies in QDO+ medium. Last column shows the false positive signal in the control.

We then focused on using microscopic techniques to identify potential interactors of MTA. We used confocal image co-localisation in conjunction with FRET-FLIM data to analyse these interactions. *Arabidopsis* protoplasts isolated from the leaves were transfected with a combination of two proteins tagged with GFP and RFP separately. In all cases, MTA was tagged with RFP at the N terminus (RFP-MTA). Prospective protein partners were tagged with GFP either on the C terminus (DDL1-GFP, HYL1-GFP, SE-GFP) or at the N terminus (GFP-CBP20, GFP-TGH). In FRET analysis a statistically significant decrease in the donor GFP lifetime caused by a transfer of energy from donor GFP to acceptor RFP indicates physical interaction between two proteins *in vivo*. This energy transfer can only occur when the acceptor and donor are within nanometres of each other. We observed that even though MTA and all the target proteins reside in the nucleus, MTA showed strong interaction only with TGH. Another observation that can be made is that with all other protein targets MTA is uniformly spread over the nucleus but in present of TGH, MTA localises to specific loci that also contain TGH. The results can be visualised in Fig 7. These data show that MTA interacts with TGH protein.

The interaction of MTA with Not2b could not be confirmed using microscopic studies as the NOT2b protein could not be stably expressed in *Arabidopsis* protoplasts and formed visible aggregates instead.

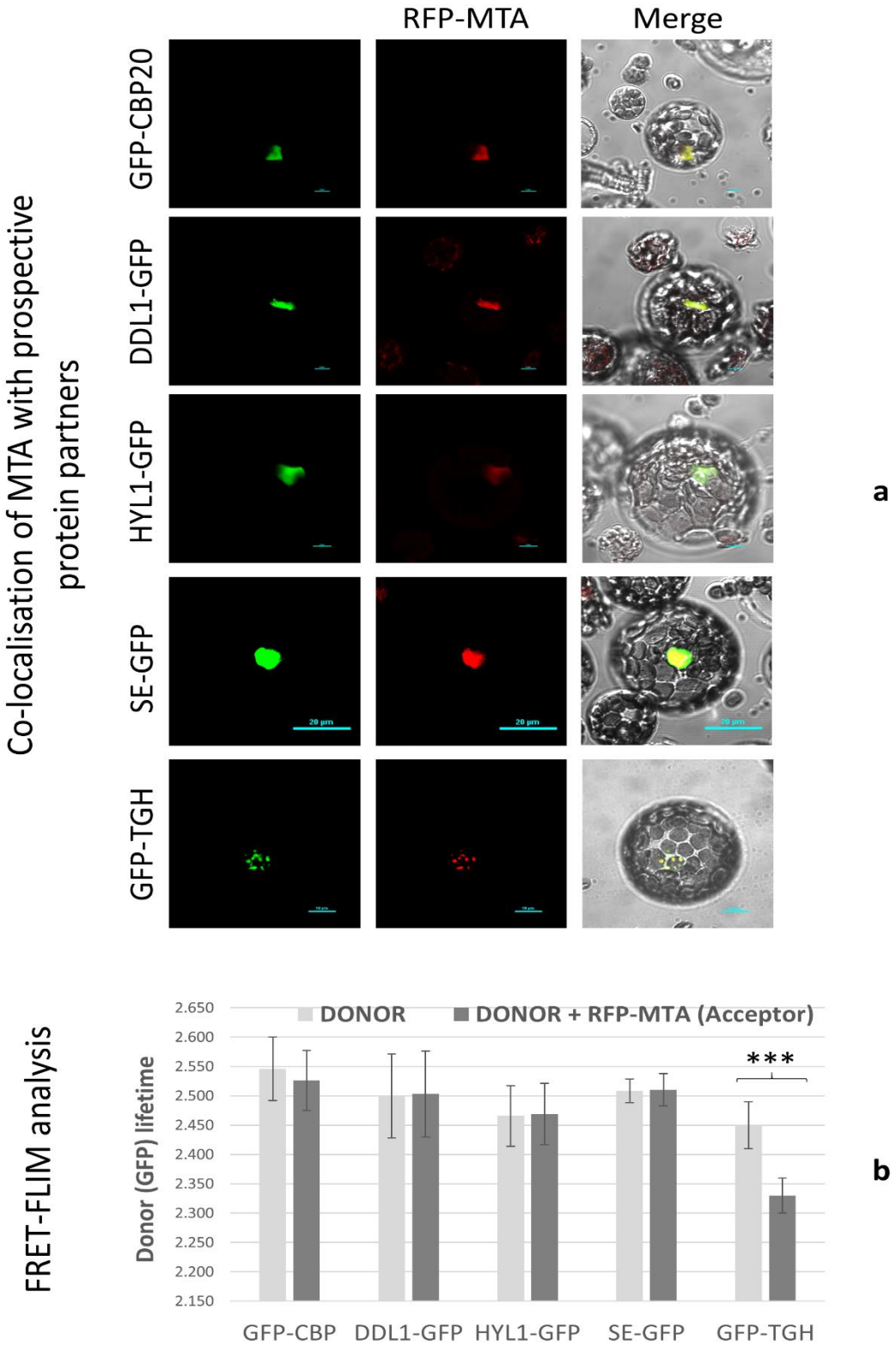

Figure 7 MTA interacts with TGH. (a) Co-localisation images show the expression of MTA (red) with target proteins (green). Right most column shows a merged image. Scale bars

are presented at bottom right. **(b)** FRET-FLIM analysis shows a decrease in GFP-donor lifetime only when donor is GFP-TGH. RFP-MTA is acceptor in all cases. *** = p-value <0.001, n = 9.

We also wanted to identify proteins interacting with MTA on a more global level. For this purpose, we used co-immunoprecipitation followed by mass spectroscopy (MS). Anti GFP antibody was used to pull down MTA-GFP and all the protein partners associated with MTA. The proteins were ranked on the basis of the number of peptide fragments (for a particular protein) identified after MS. Using this approach, we were able to identify MTA, VIR, MTB and FIP37 (proteins that make a functional complex together with MTA) as the top 4 proteins which proves the robustness of the method. Certain proteins that stand out in our data are CDC5, MOS4 associated complex proteins 3A and 3B (MAC3A/MAC3B), PRL1, CBP20 and HOS5 (Fig 8). CDC5, MAC3A/3B and PRL1 are subunits of MOS4-associated complex (MAC) and play varied roles in miRNA biogenesis[31,126–128]. HOS5 and serine/arginine rich splicing factors 40/41 (RS40/41, also identified in our data) affect pri-miRNA splicing and miRNA strand selection[129]. CBP20 and its partner CBP80 have both been shown to bind pri-miRNAs and positively affect their processing[130]. Another protein, Karyopherin Enabling the Transport of the Cytoplasmic HYL1 (KETCH1) is worth noting in our data. KETCH1 is a protein partner of HYL1 that is necessary for the nuclear localisation of HYL1 and hence proper biogenesis of miRNAs[131]. These examples link MTA to miRNA biogenesis with high significance. HOS5, RS40/41 and CBP20 are also involved in splicing of mRNAs and we know that m^6A affects splicing patterns of mRNAs in animals. Thus, these results also provide a first link between MTA and mRNA splicing in plants.

Accession number	Score	Fold Change	Protein name
AT4G10760	164	9.885	EMB1706, EMBRYO DEFECTIVE 1706, MRNAADENOSINE METHYLASE, MTA
AT3G05680	17.5	6.655	EMB2016, EMBRYO DEFECTIVE 2016, VIR, VIRILIZER
AT4G09980	16.5	6.607	EMB1691, EMBRYO DEFECTIVE 1691, METHYLTRANSFERASE B, MTB
AT3G54170	15	6.442	ATFIP37, FIP37, FKBP12 INTERACTING PROTEIN 37
AT5G19820	9	5.735	KARYOPHERIN ENABLING THE TRANSPORT OF THE CYTOPLASMIC HYL1, KETCH1
AT1G15750	6.5	5.233	TOPLESS, TPL, WSIP1, WUS-INTERACTING PROTEIN 1
AT3G58510	6.5	5.145	"DEA(D/H)-box RNA helicase family protein
AT1G80490	5.5	4.987	TOPLESS-RELATED 1, TPR1
AT3G19760	5	4.913	EIF4A-III, EUKARYOTIC INITIATION FACTOR 4A-III, RH2
AT3G16830	3.5	4.396	TOPLESS-RELATED 2, TPR2
AT3G15880	3.5	4.396	TOPLESS-RELATED 4, TPR4, WSIP2, WUS-INTERACTING PROTEIN 2
AT5G52040	3	4.197	"arginine/serine-rich splicing factor 41 (RSP41)
AT4G25500	2.5	3.925	"arginine/serine-rich splicing factor 40 (RSP40)
AT1G04510	2.5	3.871	MOS4-associated complex 3A (MAC3A)
AT1G09770	2	3.595	cell division cycle 5 (CDC5)
AT5G53060	1	2.731	RNA-binding KH domain-containing protein (HOS5)
AT2G33340	1	2.731	MOS4-associated complex 3B (MAC3B)
AT4G15900	0.5	2.011	pleiotropic regulatory locus 1 (PRL1)
AT5G44200	0.5	2.011	CAP-binding protein 20 (CBP20)
AT2G21660	6	0.4578	GLYCINE-RICH RNA-BINDING PROTEIN 7 (ATGRP7)

Figure 8 MTA interactome. A list of the most abundant proteins identified by co-immunoprecipitation followed by mass spectroscopy. MTA-GFP was used as a bait to pull down the proteins. First 4 most abundant proteins are bona fide members of *Arabidopsis* methyltransferase complex. Other important miRNA biogenesis factors like CDC5, MAC3A/3B and CBP20 can also be seen. Results shown are obtained from two biological replicates.

m^{6}A affects mRNA metabolic processes like splicing and alternative polyadenylation[106,107,132,133]. Although performed in animal systems, these studies indicate that m^{6}A is deposited on RNA co-transcriptionally. No evidence of co-transcriptional activity of MTA in plants was available so far. We collaborated with Tomasz Gulanicz in our lab and Dr. Dariusz Smolinski (Centre for Modern Interdisciplinary Technologies, Nicolaus Copernicus University, Torun) to test whether MTA could interact with RNA Pol II. We used proximity ligation assay (PLA) in fixed nuclei of MTA-GFP plants to determine this interaction *in vivo*. Using PLA, we could observe positive signals only in MTA-GFP nuclei but not in GFP control. These results were obtained for RNA Pol II phosphorylated at Serine 2 and Serine 5 (Ser2 and Ser5) individually. Thus, our data show that MTA is associated with RNA Pol II since early stages of transcription and can methylate pri-miRNAs (among other RNA Pol II transcripts) co-transcriptionally. These results are summed in Figure 9.

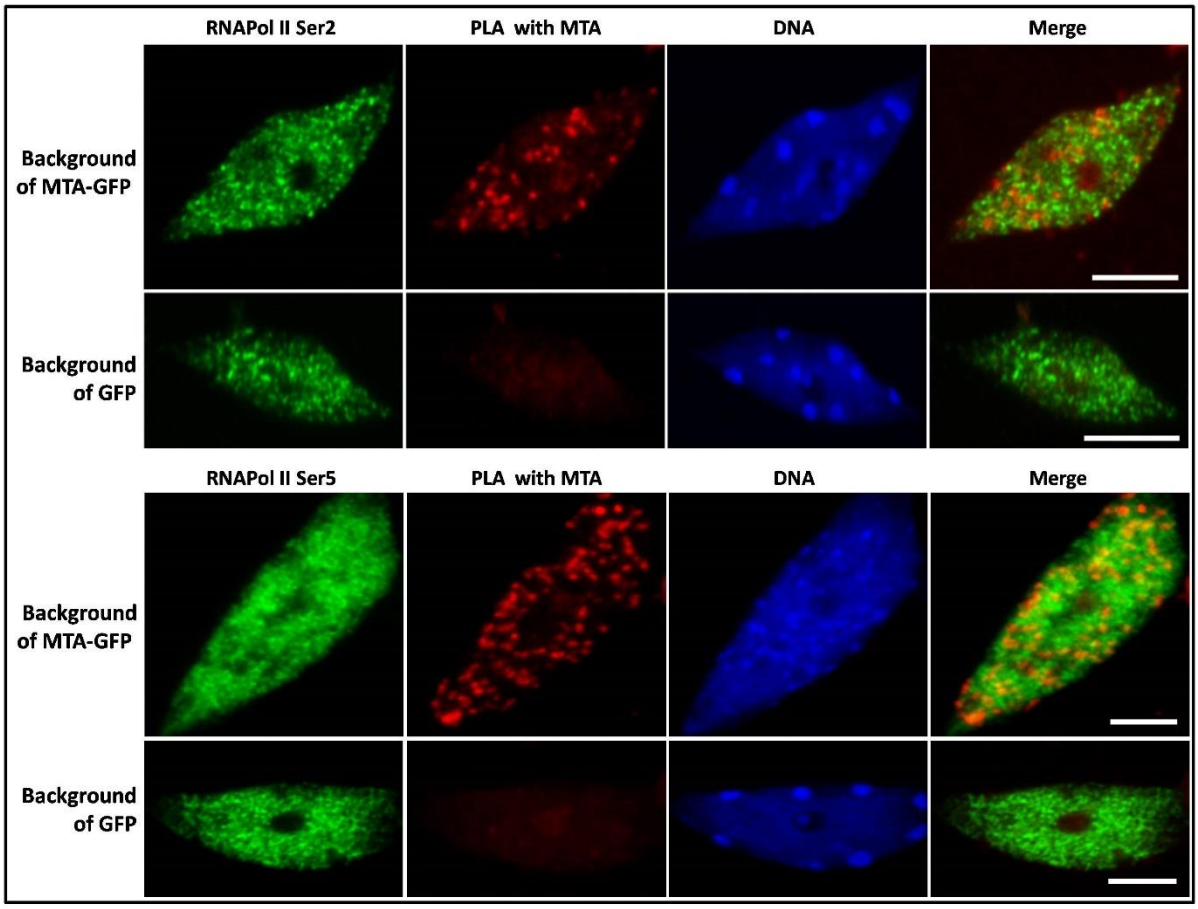

Figure 9 MTA interacts with RNA Pol II. Proximity Ligation assay was used to investigatese the interactions between MTA and RNA Pol II. Interactions were analysed with

RNA Pol II phosphorylated at Ser2 and Ser5. Red spots in the second column indicate positive PLA signals and can be observed only in cells containing the MTA-GFP transgene but not in control cells expressing GFP only. RNA Pol II is represented in green. DNA is stained with HOECHST (blue). Scales bars (white) = 5µm.

5.5 MTA acts upstream of TGH and both are needed for proper Microprocessor assembly

Since MTA interacts with RNA Pol II and TGH both we wanted to know whether the interactions of MTA and TGH have any effect on the methylation status of pri-miRNAs. To test this, we performed m^{6}A-IP followed by RT-qPCR in WT and *tgh-1* mutant plants. We did not observe a significant difference in the m^{6}A methylation status of pri-miRNAs in *tgh-1* mutant (Fig 10). These data confirm that MTA acts co-transcriptionally and upstream of TGH in miRNA biogenesis.

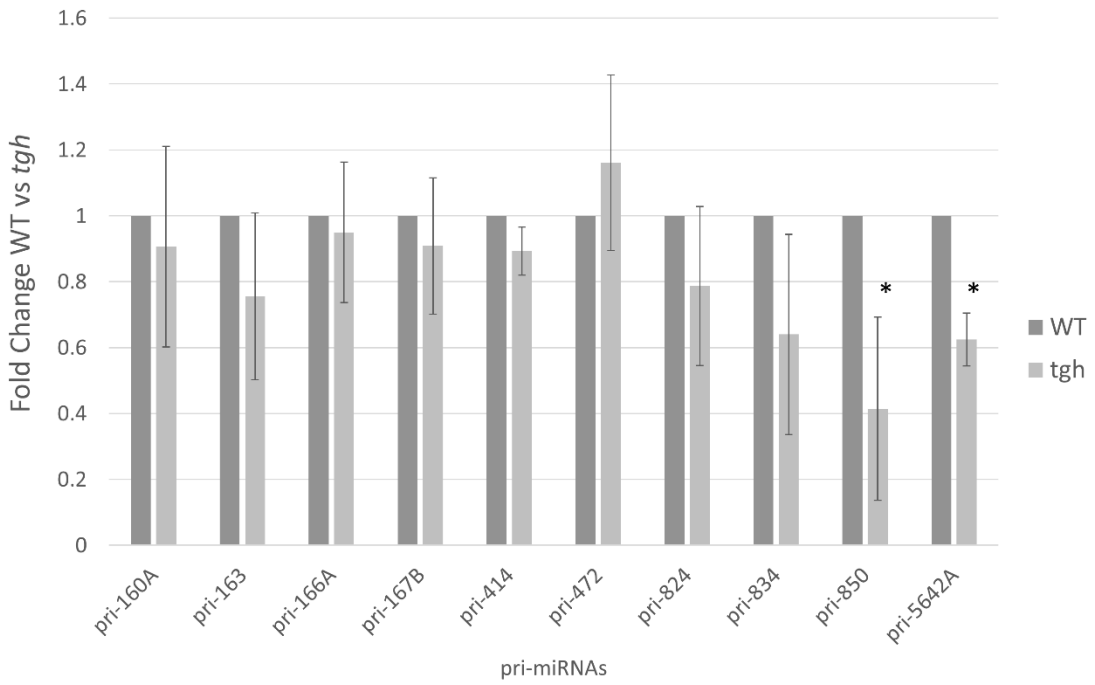

Figure 10 m^{6}A methylation status of pri-miRNAs in *tgh-1* mutant. Changes in the m^{6}A level of pri-miRNAs in *tgh-1* mutant as compared to WT mutants are presented. 10 pri-miRNAs found in m^{6}A-IP seq data were analysed and only 2 were found to have statistically significant reduction in m^{6}A levels. Bars represent standard deviation, * = p-value < 0.05, n =3.

Since we identified MTA and TGH interactions in WT plants and we already identified the inability of HYL1 to bind pri-miRNAs efficiently in the *mta* mutant background we investigated whether these observable changes affect miRNA biogenesis. Since TGH is known to promote HYL1 binding to pri-miRNAs and also enhance DCL1 activity[42], we asked whether the absence of MTA or TGH could affect association of HYL1 and DCL1 with RNA Pol II. An immunolocalization study done by Tomasz Gulanicz showed a significant decrease in co-localization of DCL1, and HYL1 with RNA Pol II in both *mta* and *tgh* mutants (Fig 11). This decrease was seen in the case of RNA Pol II phosphorylated at either Ser2 or Ser5, indicating that the co-transcriptional Microprocessor assembly is hampered from the early stages of *MIR* genes transcription. These observations provide us with the idea about how MTA and TGH are both necessary for proper assembly of Microprocessor.

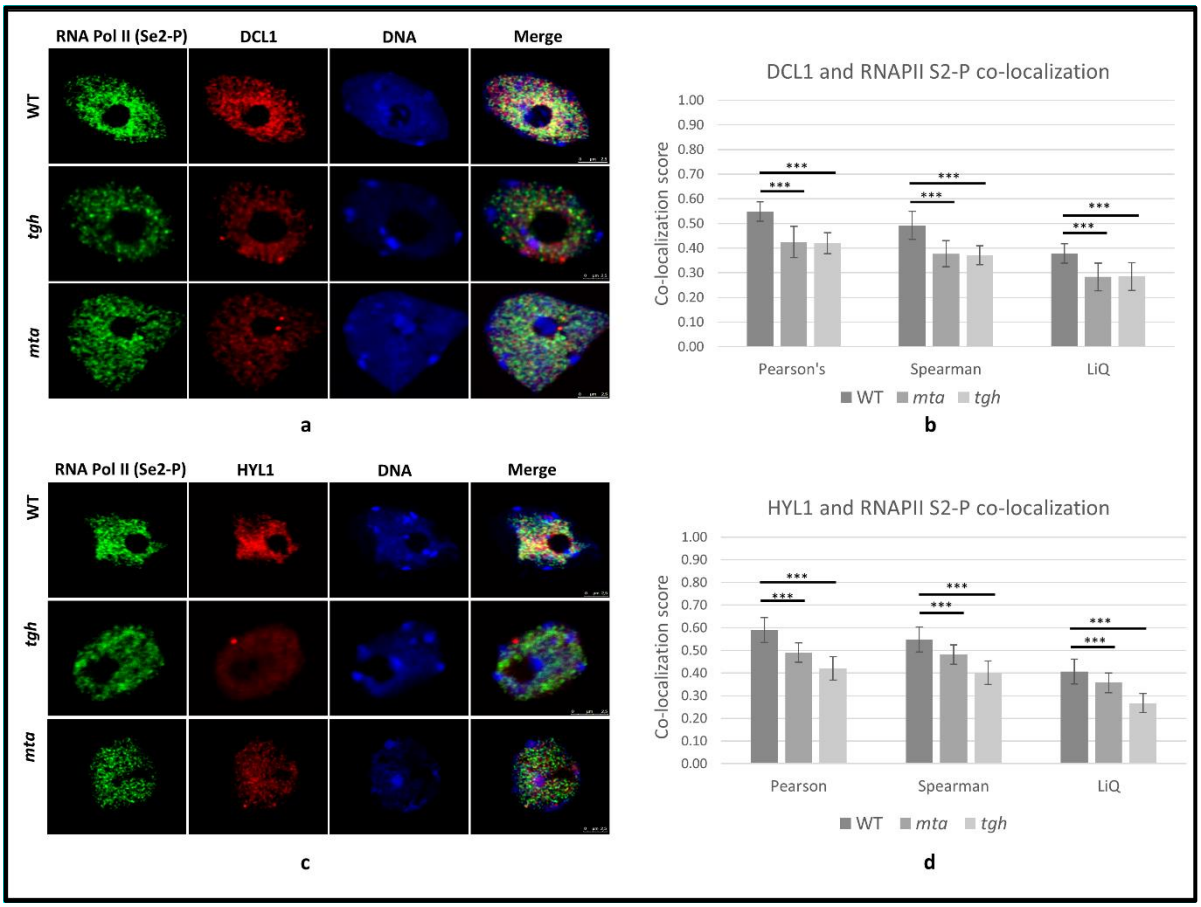

Figure 11 DCL1 and HYL1 co-localization with RNA Pol II in *mta* and *tgh* mutants. (a) Nuclei with reduced co-localization of DCL1 with RNA Pol II in *mta* and *tgh* can be seen. RNA Pol II (green), DCL1 (red) and DNA (blue) **(b)** Various statistical parameters are used to

quantify the reduction in co-localization. **(c)** Nuclei with reduced co-localization of HYL1 with RNA Pol II in *mta* and *tgh* can be seen. RNA Pol II (green), HYL1 (red) and DNA (blue) **(d)** Various statistical parameters are used to quantify the reduction in co-localization. *** = p-value <0.001, n = 50

5.6 MTA regulated miR393b biogenesis affects auxin response

So far, we have inspected the inter-relation between two very critical RNA metabolic pathways of miRNA biogenesis and m^6A methylation. It was thus incumbent for us to know the physiological effects of this cross talk. Since auxin defects in mutants of m^6A methylation pathway have already been reported we focused on the same[94]. We started by examining the auxin response of *mta* hypomorphic plants. Using a *proDR5:GUS* (in *mta* and WT background) we tested auxin induction in 14-days old seedlings. Indeed, GUS expression was found to be much lower in *mta* background as compared to WT plants (Fig 12a).

miR393b is a key regulator in auxin response pathway and we detected that miR393b expression is significantly reduced in *mta* hypomorphic mutant from our sRNA sequencing data. Using RT-qPCR, we also found that pr-miR393b is m^6A methylated and MTA binds to the pri-miR393b (Fig 12b). We counter tested this evidence using an orthogonal approach in *Nicotiana* system. MTA CDS was used to prepare constructs of a functional MTA gene and a non-functional gene. In animals, a DPPW motif is required for catalytic action of METTL3[134]. This motif is conserved in animals and *Arabidopsis*[134]. For our non-functional MTA construct we modified the aspartic acid at position 482 to alanine (D482A) in the catalytic DPPW motif. This should lead to the expression of a catalytically inactive MTA protein referred to as ΔMTA. We co-transfected *Nicotiana* leaves with a vector expressing pri-miR393b and either the functional MTA or ΔMTA construct. We then monitored the production of mature miR393b from such leaves. We observed that when we expressed pri-miR393b with functional MTA, miR393b production was enhanced by 2.3 folds while this effect could not be observed in case of ΔMTA (Fig 12c).

Thus, we provide conclusive evidence that MTA is directly involved in the biogenesis of miR393b and in its absence the reduced level of miR393b causes auxin insensitivity in *mta* hypomorphic mutant.

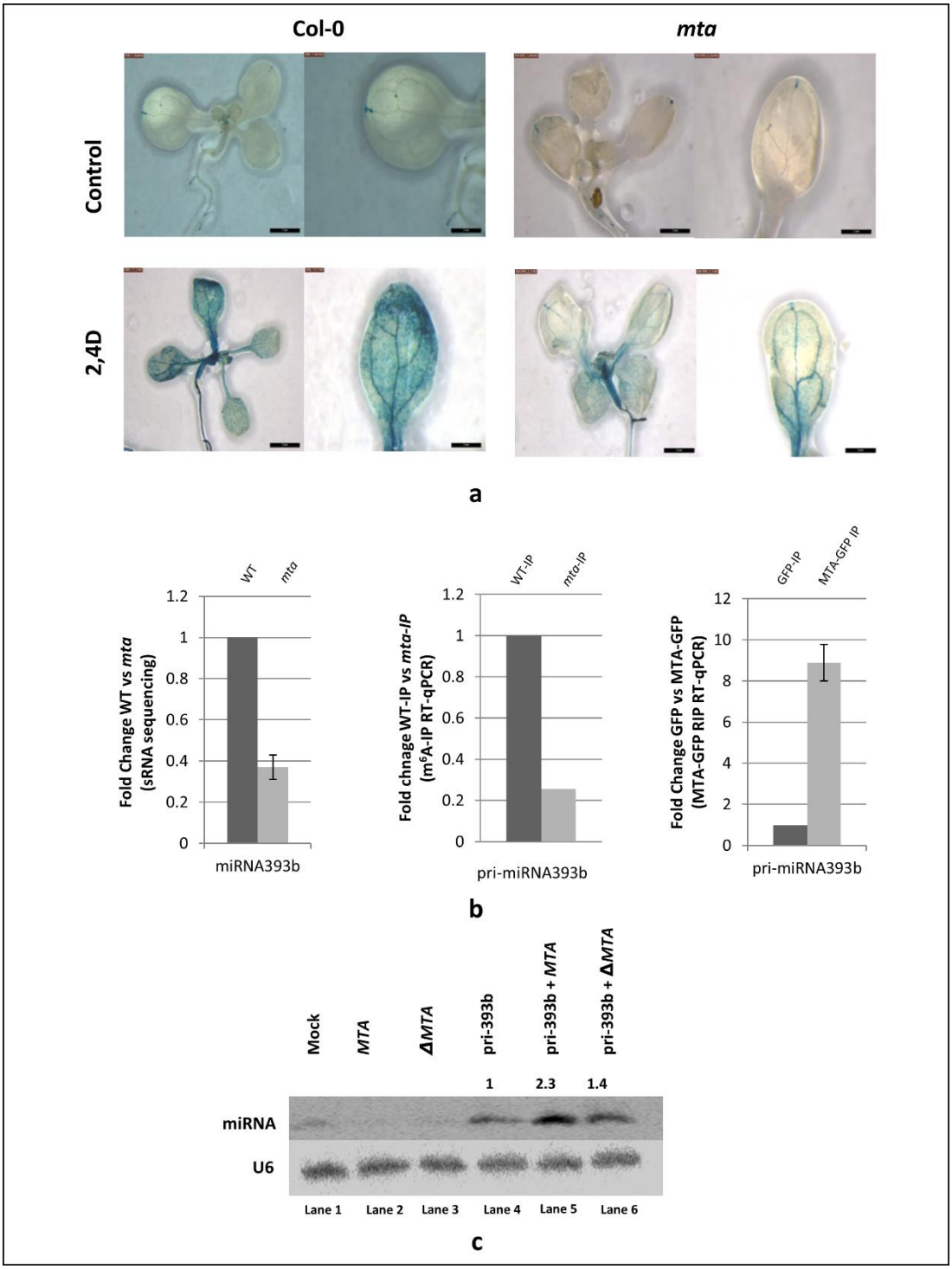

Figure 12 MTA influences auxin response vis miR393b. (a) Expression of Auxin responsive reporter gene *proDR5:GUS* is shown in WT and *mta* backgrounds. After induction with auxin (2,4 Dichlorophenoxyacetic acid; 2,4D), *mta* plants show much less GUS expression as compared to WT plants. Scale bars (bottom right) = 2mm. **(b)** Graphs (from left to right) show the reduced level of miR393b in *mta* mutant, low methylation status of pri-miRNA in *mta*

mutant and enrichment of pri-miR393b in MTA-GFP sample meaning that MTA binds to pri-miR393b. Error bars represent standard deviation. **(c)** Northern blot analysis of miR393b obtained from different conditions. Lane 1 shows mock transformation. Lane 2 and 3 are samples transfected only with MTA and ΔMTA constructs. Lane 4 represents transfection only with pri-miR393b and presents a basal expression level of miR393b. Lane 5, where pri-miRNA is expressed with MTA shows a 2.3-fold increase in miR393b production. In lane 6, ΔMTA cannot enhance the expression of miR393b as catalytically active MTA could. U6 serves as loading control.

6 Discussion

6.1 Direct MTA-RNA interactions and its effect on miRNA biogenesis

Among the many diverse roles of m^6A, its function in miRNA biogenesis has been very obscure so far, especially in case of plant systems. In animals, it was reported that m^6A methylation by methyl transferase like 3 (METTL3), a homolog of MTA, promotes processing of pri-miRNAs in mammals[135]. The lack of METTL3 leads to reduction in levels of mature miRNAs while pri-miRNAs tend to accumulate. It was later reported that a m^6A reader, Heterogeneous Nuclear Ribonuclear Protein A2B1 (HNRNPA2B1), facilitates the recruitment of animal microprocessor component DGCR8 to the pri-miRNAs for their efficient processing[136]. miRNA biogenesis in both plants and animals share some similarities but differ in the fact that in plants both pri-miRNA cleavage steps are carried out in the nucleus by one enzyme DCL1. While in animals one pri-miRNA cleavage takes place in the nucleus and second in the cytoplasm, and are catalysed by two different enzymes DROSHA and Dicer, respectively[137].

Our first experiment to test the miRNA levels revealed downregulation of mature miRNAs in *mta* mutant plants. Upon testing the pri-miRNA levels, we found that pri-miRNAs generally tend to accumulate in this mutant as compared to WT. These results are similar to those seen in animal system and indicate a hampered processing of pri-miRNAs. In this regard, *mta* plants bear also close resemblance to plant mutant lines of proteins involved in pri-miRNA processing for eg, *hyl1* and *se*[39–41]. On the contrary, plant mutant of a protein that acts at a later stage of miRNA biogenesis, *hen1,* does not show accumulation of pri-miRNAs[21], although miRNA downregulation can be observed in this mutant. While the abundance and omnipresence of m^6A served as a seed of thought for this thesis, it also presented our next challenge. Since m^6A is present in almost all RNAs, including mRNAs, it was important to know whether pri-miRNAs carry the m^6A mark and if so, is their methylation a product of MTA action. m^6A-IP followed by NGS provided us with evidence that allowed us to identify a set of pri-miRNAs that carry

this mark. Since pri-miRNAs are significantly less abundant than mRNAs in the cell, they are often detectable in sequencing data at a very low level or not at all. Keeping these constraints in mind, we were still able to identify 11 pri-miRNAs as positively m^6A methylated. Our next aim was to prove that this methylation was a direct result of MTA activity. We used MTA-GFP RIP to look into this possibility. RT-qPCR after RIP clearly showed enrichment of pri-miRNAs in MTA-GFP samples as compared to GFP control. These data suggest that MTA directly binds to pri-miRNAs and methylates them, hence our observation of altered miRNA biogenesis is a direct result of MTA action. So far, our data are in close agreement with data obtained from animal studies. In case of animals, crosslinking immunoprecipitation was used to show that METTL3 binds to pri-miRNAs. METTL3 binding site and the m^6A methylation site were also shown to contain the GGAC motif[135]. Although we have an indication that the GGAC/AGAC motif is present in plant pri-miRNAs (Fig 2e), whether these motifs are preferentially methylated by MTA needs further investigation.

As established in this thesis, the lack of MTA causes a general accumulation of pri-miRNas while miRNA accumulate to a lower level. However, we do find some outliers in our data. 9 miRNAs were such whose levels were found to be more in *mta* mutant as compared to WT plants. When we looked at their corresponding pri-miRNAs (in our RT-qPCR data), we found that out of the 8 detectable pri-miRNAs, only 2 had changes in their accumulation at statistically significant level. These were pri-miR5026 and pri-miR3440b. While pri-miR5026 is down regulated in *mta* mutant, pri-3440b is upregulated. Both these miRNAs are up regulated in *mta* mutants. There are also 29 pri-miRNAs that we found to be down regulated in our data. When we looked for the levels of corresponding miRNAs for these 29 pri-miRNAs we found that only 9 had statistically significant changes in their accumulation levels. All of these 9 miRNAs were down regulated in *mta* mutant. For the rest 20 we did not either see statistical changes or the mature miRNA was not detected in our sRNA sequencing data. As a possible cause for these exceptions, we reason that they could be caused because of the complex network of metabolic pathways that influence miRNA biogenesis. The processing of pri-miRNAs is affected by cellular processes like splicing, alternative polyadenylation and degradation efficiency[83,138–141]. These processes in turn can be affected by RNA structure, which is influenced by m^6A (discussed further below). Hence, we hypothesize that the changes in the m^6A methylation status affects miRNA biogenesis in more ways than one.

Another intriguing aspect of m^6A and miRNA is presented by the regulation of m^6A methylation by miRNA. Researchers have shown that animal miR423-3p and miR1226-3p regulate the levels of m^6A methylation in their target genes[142]. The authors also show that the miRNAs positively affect the binding of METTL3 to their targets[142]. These data show that the role of m^6A in miRNA biogenesis or, miRNA related metabolism in general, is not a one-way street. m^6A can affect miRNA biogenesis, but miRNAs can also affect m^6A deposition. These data can serve as a starting point for future studies that have the possibility of analysing this crosstalk between miRNAs and m^6A methylation in plants.

6.2 m^6A and RNA structure

Another intriguing issue dealt with the problem concerning if and how the presence/absence of m^6A affects secondary structure of pri-miRNAs in *Arabidopsis*. As mentioned in the introduction, structural features of pri-miRNAs are essential for proper DCL1 cleavage. Studies have shown the importance of imperfect base pairing in the lower stem region of pri-miRNAs that are processed according to the so-called base-to loop mechanism[20]. A bulge of ~15nt between the miRNA/miRNA* duplex and the less structured end of pri-miRNAs is often considered to be a determining factor in pri-miRNA cleavage[15,16]. In this canonical pathway, first cut by DCL1 happens at the base of the stem loop and second cut near the loop. However, a loop to base mechanism was also demonstrated and notably instead of the sequence, the secondary structure of pri-miRNA was found to be more important for determination of such processing[17]. Clearly, pri-miRNA structure plays an important role in their processing.

The PIP-seq technique is able to provide us the information about not only the secondary structure of the target RNAs, but also the protein interaction profiles of the same. A comparison between the four libraries prepared after treating the samples with structure specific RNAse with or without proteinase K treatment gives us a profile of RNA structure. One such study performed in nuclear fraction of *Arabidopsis* revealed that the secondary structure of RNA was inversely co-related to the protein binding profile[143]. The CDS region of mRNAs was found to be enriched in the fraction bound by proteins and has less secondary structures while the 5' and 3' UTRs have less proteins bound with more complex structure[143]. The data analysed as a part of this thesis, shows that in absence of MTA and hence m^6A, pri-miRNAs cannot fold into proper hair pin loops, especially in the region containing miRNA. Interestingly, these results are in contrast to the studies done in animal mRNAs where presence of m^6A is detrimental to

the loop formation. In fact, the presence of m^6A leads to the disruption of hairpin-loop allowing for more easy access to RNA binding proteins[117,123]. What is more, the de-stabilizing effect can be seen only in the paired regions of RNA while in single stranded regions m^6A acts as a stabilizing modification[122]. The data from structural probing presented in this thesis suggest that the presence of m^6A rather stabilizes the secondary structures of pri-miRNAs in the pre-miRNA region. Alternative way is that the lack of m6A in the region outside the pre-miRNA structure may indirectly affect the miRNA/miRNA* stem-loop formation. The mechanism behind this opposite effect in plant miRNAs needs to be investigated and may need information regarding the location of m^6A modification in pri-miRNAs at a single base resolution.

m^6A induced structural changes, m^6A switch, could also be at the bottom of the data outliers observed in this study. The structure of RNA is altered by m^6A in varied ways, depending on where the methylation is present. While a global destabilizing effect on m^6A has been the major observation in this area, there is evidence of m^6A stabilizing RNA structure. It has been shown that when m^6A is present in an unpaired region it stabilizes nearby helices[122]. A study also showed that when m^6A has a bulge in the 5' vicinity and in presence of Mg^{2+}, it stabilizes the entire RNA structure[144]. It is clear that the location of m^6A methylation plays an equally important role in determining the overall structure of RNA as the modification itself. It is possible that in some specific cases, the lack of m^6A could favor secondary structure formation, hence resulting in better miRNA production from such precursors. Also, as mentioned above, pri-miRNAs are subject to various post-transcriptional processes. Various RNA binding proteins could possibly lose or gain access to pri-miRNA based on their structure. For example, binding of pri-miR472 is not affected in *mta* mutant. Interestingly, when we looked at the 2D structural profile of pri-miR472, we found that while the overall structure of the precursor is more distorted in *mta* mutant, the miRNA still resides in a double stranded region (Fig 13). This may allow binding of HYL1 to the precursor while the irregular stem loop could hamper DCL1 activity.

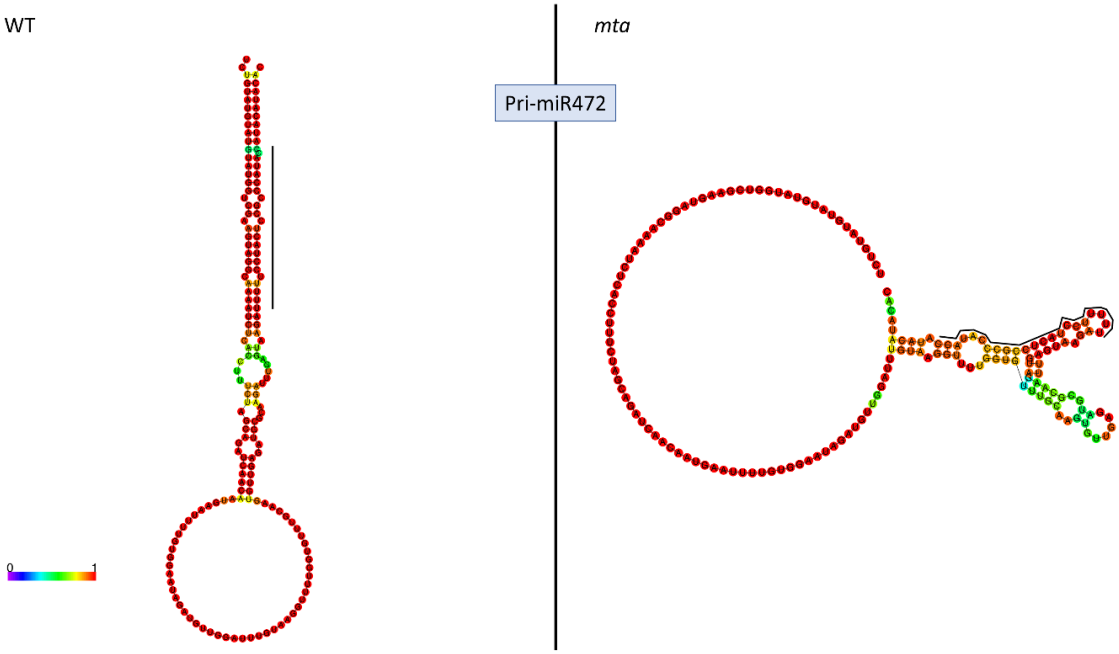

Figure13 A 2D structural analysis of pri-miR472 is presented. The region in which miRNA is contained is marked by a black line. Color bar represents the probability score of a base to be in the single or double base paired state as calculated by the folding algorithm. Analysis performed in co-operation with Dr Brian Gregory laboratory by Xiang Yu.

While we identified transcripts that contain m^6A mark, we did not obtain data at single nucleotide resolution. Data at single nucleotide resolution is the next step forward as the knowledge of the location where a pri-miRNA carries the m6A mark would help us predict the structural changes associated with it better. These observations provide a platform for future studies investigating pri-miRNA structure in relation to m^6A and pri-miRNA.

6.3 The MTA interactome and its impact on miRNA biogenesis

Protein-protein interactions between MTA and other potential interactors especially those involved in miRNA biogenesis can also play a role in the observable effects of m^6A methylation. In animals, Microprocessor component DGCR8 interacts not only with the m^6A reader HNRNPA2B1 but with METTL3 as well[136,145,146]. We asked whether MTA itself could interact with one or more proteins involved in miRNA biogenesis in plants. Our co-localization and FRET data showed clear interaction of MTA with TGH. This is an interesting finding, as

TGH is a protein that facilitates DCL1 activity and also contributes to the interaction between HYL1 and pri-miRNAs. *tgh* mutant also follows the pattern of pri-miRNA accumulation and miRNA downregulation[42]. Upon comparison of our sRNA sequencing data with that from a previously published data from *tgh* mutants[42], we found a 45% overlap between the miRNAs. These data sets were from two different tissues; hence we believe that given the same tissue, this overlap could be even more significant. Since, we did not see any significant changes in m^6A levels in pri-miRNAs in *tgh* mutant and we show that MTA interacts with RNA Pol II we concluded that MTA must act upstream of TGH. Clearly, the interaction between MTA and TGH is crucial for proper regulation of miRNA biogenesis. Whether TGH is attracted to pri-miRNAs by the structural changes caused by m^6A or by its direct association with MTA needs further investigations.

A more global overview of MTA interactome was provided by our mass spectrometry data. We identified four core proteins of the methyltransferase complex as the top interactors with MTA showing that our data was robust. Several proteins involved in miRNA biogenesis were identified in our mass spectrometry data like CDC5, MAC3A/3B, HOS5 and CBP20. While all these proteins play some defined roles in miRNA biogenesis, the stages at which they affect the same are varied and guided the decision to investigate their interaction with MTA via other techniques. CDC5 is a transcription factor and in its absence pri-miRNA levels were found to be lower[31], opposite to what is seen in hypomorphic *mta* mutant. CDC5 and MTA both associate with RNA Pol II, but while CDC5 could be considered a protein that binds to *MIR* specific promoters, MTA acts at a global scale not just for *MIR* transcripts. Worth noting is that other components of MAC complex, PRL1 and MAC3A/3B were also found in our data and are involved in miRNA biogenesis. PRL1 and MAC3A/3B do not affect *MIR* transcription but bind to pri-miRNAs and are thought to regulate the stability of pri-miRNAs[127,128].

Similarly, HOS5, RS40/41 and CBP20 are all associated with splicing in mRNAs as well as miRNA biogenesis[129,130]. Although, these data provide first insight into the possible connection of m^6A methylation with pre-mRNA splicing in plants, this connection has been studied in animal systems. Notably, reader proteins from hnRNP and YTHDC families have been associated with splicing. Presence of m6A near splice sites promotes exon inclusion by affecting HNRNPG binding which further affects RNA Pol II occupancy via direct protein-protein interaction[133]. Another reader, YTHDC1 also promotes exon inclusion by facilitating binding of splicing enhancer-binding SR protein 3 (SRS3) and at the same time blocking access

to SRS10[147]. Interestingly, m^{6}A demethylases Fat Mass and Obesity- associated protein (FTO) and ALKBH5 also influence splicing. Lack of FTO also leads to exon exclusion via SRSF2 binding of mRNAs[106]. ALKBH5 has been associated with production of longer 3' UTRs in mRNAs owing to the proper removal of m^{6}A marks. In its absence the methylated transcripts have shorter 3'UTRs and are rapidly degraded[132]. Since HOS5, RS40/41 and CBP20 are all associated with splicing in mRNAs as well as miRNA biogenesis, our data provide novel insights into the connections between plant MTA/m^{6}A methylation and critical RNA metabolic processes. Any study regarding the MAC subunits or the proteins connecting miRNA biogenesis and mRNA splicing needs to be done in a holistic manner and would need time and effort beyond the scope of this thesis. However, we have to admit that we did not find TGH in our mass spectrometry data. We reason that the interaction between MTA and TGH could be transient and it was not feasible to catch it in mass spectroscopy experiment.

m^{6}A deposition has been shown to be co-transcriptional in animals as evident by the several co-transcriptional events regulated by it. Our results showing interaction between RNA Pol II and MTA provide first evidence of co-transcriptional m^{6}A methylation in plants. Similarly, pri-miRNAs are also processed co-transcriptionally in both animal and plant systems[148–150]. By identifying the interaction between MTA and TGH that precedes (and is vital for) the Microprocessor assembly, we provide novel evidence of interconnection between pri-miRNA processing and m^{6}A methylation. All these data put together allowed us to put together a model to depict MTA's role in *Arabidopsis* miRNA biogenesis. According to our data, MTA acts co-transcriptionally and possibly depositing m^{6}A on nascent pri-miRNAs. Next, TGH is recruited to the pri-miRNAs, either by its direct interaction with MTA or by a yet unknown reader protein that recognizes m^{6}A. The recruitment of TGH acts as a pivotal step for the assembly of the rest of the Microprocessor over the pri-miRNA. These steps ensure the proper processing of pri-miRNAs and miRNA production. Fig 14 depicts the model graphically.

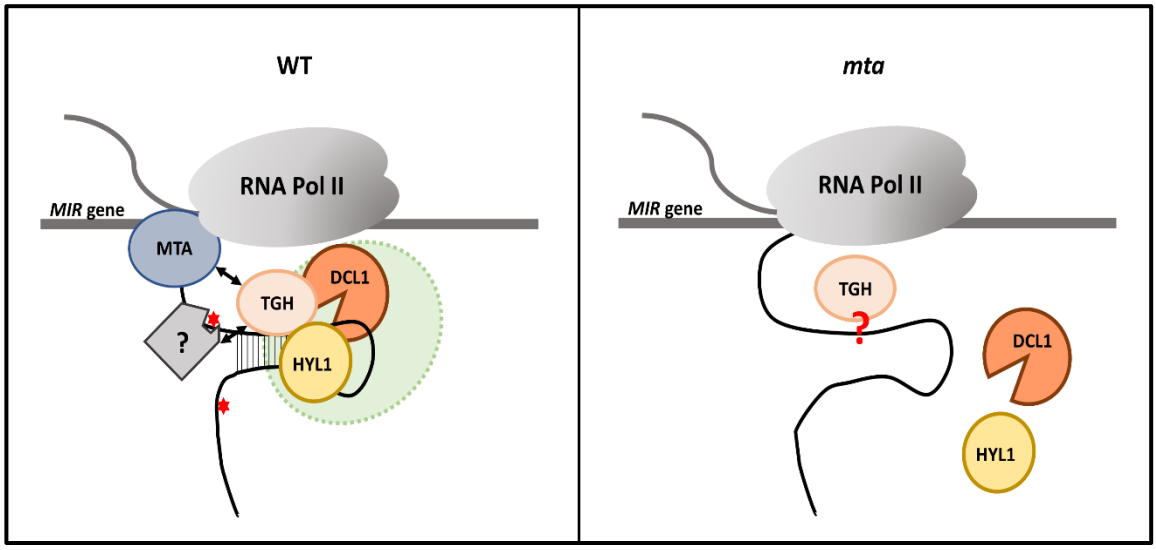

Figure 14 Model depicting the role of MTA in pant miRNA biogenesis. (a) In wild type plants, MTA marks pri-miRNAs co-transcriptionally (red star depicts m^6A). TGH is recruited to the pri-miRNA either via its interaction with MTA or with a yet unknown m^6A reader protein (marked by ?). These interactions lead to efficient Microprocessor assembly. **(b)** *mta* plants lack MTA and hence no m^6A on pri-miRNAs. Pri-miRNAs lose their structural features but whether TGH can still be recruited to pri-miRNAs is not known (marked by red question mark). These events lead to inefficient binding of HYL1 to pri-miRNAs and less efficient Microprocessor assembly.

6.4 Modulation of auxin response by MTA via miR393b

As mentioned in the introduction section of this thesis, auxin signalling is one of the pathways that is affected by m^6A methylation. Mutants with lower levels of m^6A have defects in the auxin signalling[94]. It is known that miR393 is a key player in auxin signalling pathway[74,76]. In *Arabidopsis* there are two genes encoding miR393, *MIR393A* and *MIR393b*. miR393a is dominantly expressed in the roots while miR393b is expressed in the aerial parts. miR393b is the miRNA responsive to auxin signalling. It targets four members of the Transport Inhibitor Response 1/Auxin Signalling F-Box1 Auxin receptor (TAAR) clade. TAAR proteins are responsible for the degradation of Auxin/Indole-3-Acetic Acid (AUX/IAA) transcriptional repressor protein family. Ultimately, the degradation of AUX/IAA repressors allows for transcription of auxin responsive genes via activation by Auxin Response Factors (ARF)[74,76].

This presented us an opportunity to test if the decreased level of miR393b in *mta* plants (as shown by our sRNA sequencing) was caused by reduced MTA/m^{6}A levels. Indeed, our data showed that pri-miR393b is m^{6}A methylated by MTA. Our experiment with co-expression of MTA with pri-miR393b in *Nicotiana* clearly demonstrated that MTA is necessary for proper production of miR393b. It is to be noted that miR393b is not the only miRNA involved in auxin signalling. miR160, miR167 and miR847 are also involved in auxin signalling and homeostasis pathways[151]. miR160a and miR167b were also found to be methylated and bound by MTA in our study. Hence it is clear that MTA can affect auxin signalling by more means than one. Further studies need to be undertaken to uncover the full extent of MTA's effect on auxin signalling mediated by miRNAs. Not to mention that a direct effect on biogenesis of proteins involved in auxin signalling (caused by MTA/m^{6}A related influences on the mRNAs of ARFs) cannot be excluded. These results provide novel insight into how the regulation of miRNA biogenesis by MTA has functional consequences that affect plant growth and development. It is easy to imagine that the influence of MTA on biogenesis of other miRNAs can lead to many significant cellular and physiological effects. Thus, the role of MTA/m^{6}A methylation is not limited to just mRNA metabolism but extends to the metabolism of other ncRNAs and as described in this thesis, miRNAs among them.

7 References

1. Higgs, P. G. & Lehman, N. The RNA World: Molecular cooperation at the origins of life. *Nature Reviews Genetics* **16**, 7–17 (2015).

2. Wightman, B., Ha, I. & Ruvkun, G. Posttranscriptional regulation of the heterochronic gene lin-14 by lin-4 mediates temporal pattern formation in C. elegans. *Cell* **75**, 855–862 (1993).

3. Lee, R. C., Feinbaum, R. L. & Ambros, V. the C. elegans\rheterochronic gene lin-4 encodes small RNAs with antisense\rcomplementarity to lin-14. *Cell* **75: 843**–**85**, 843–854 (1993).

4. Reinhart BJ1, Slack FJ, Basson M, Pasquinelli AE, Bettinger JC, Rougvie AE, H. & HR, R. G. The 21-nucleotide let- 7 RNA regulates developmental timing in Caenorhabditis. *Nature* **403**, 901–6 (2000).

5. Pasquinelli, A., Reinhart, B., Slack, F., Maller, B. & Ruvkun, G. Conservation across animal phylogeny of the sequence and temporal regulation of the 21 nucleotide C. elegans let-7 heterochronic regulatory RNA. *Nature* **408**, 86–89 (2000).

6. Llave, C., Kasschau, K. D., Rector, M. A. & Carrington, J. C. Endogenous and silencing-associated small RNAs in plants. *Plant Cell* **14**, 1605–1619 (2002).

7. Reinhart, B. J., Weinstein, E. G., Rhoades, M. W., Bartel, B. & Bartel, D. P. MicroRNAs in plants. *Genes Dev.* **16**, 1616–1626 (2002).

8. Park, M. Y., Wu, G., Gonzalez-Sulser, A., Vaucheret, H. & Poethig, R. S. Nuclear processing and export of microRNAs in Arabidopsis. *Proc. Natl. Acad. Sci. U. S. A.* **102**, 3691–3696 (2005).

9. Xie, Z. Expression of Arabidopsis MIRNA Genes. *Plant Physiol.* **138**, 2145–2154 (2005).

10. Griffiths-Jones, S., Saini, H. K., van Dongen, S. & Enright, A. J. miRBase: tools for microRNA genomics. *Nucleic Acids Res.* **36**, D154–D158 (2007).

11. Kim, Y. J. *et al.* The role of Mediator in small and long noncoding RNA production in Arabidopsis thaliana. *EMBO J.* **30**, 814–822 (2011).

12. Megraw, M. *et al.* MicroRNA promoter element discovery in Arabidopsis. *RNA* **12**, 1612–1619 (2006).

13. Zhao, X., Zhang, H. & Li, L. Identification and analysis of the proximal promoters of microRNA genes in Arabidopsis. *Genomics* **101**, 187–194 (2013).

14. Szarzynska, B. *et al.* Gene structures and processing of Arabidopsis thaliana HYL1-dependent pri-miRNAs. *Nucleic Acids Res.* **37**, 3083–3093 (2009).

15. Song, L., Axtell, M. J. & Fedoroff, N. V. RNA secondary structural determinants of miRNA precursor processing in Arabidopsis. *Curr. Biol.* **20**, 37–41 (2010).

16. Werner, S., Wollmann, H., Schneeberger, K. & Weigel, D. Structure determinants for accurate processing of miR172a in Arabidopsis thaliana. *Curr. Biol.* **20**, 42–48 (2010).

17. Bologna, N. G., Mateos, J. L., Bresso, E. G. & Palatnik, J. F. A loop-to-base processing mechanism underlies the biogenesis of plant microRNAs miR319 and miR159. *EMBO J.* **28**,

3646–56 (2009).

18. Cuperus, J. T. *et al.* Identification of MIR390a precursor processing-defective mutants in Arabidopsis by direct genome sequencing. *Proc. Natl. Acad. Sci. U. S. A.* **107**, 466–471 (2010).

19. Mateos, J. L., Bologna, N. G., Chorostecki, U. & Palatnik, J. F. Identification of microRNA processing determinants by random mutagenesis of Arabidopsis MIR172a precursor. *Curr. Biol.* **20**, 49–54 (2010).

20. Kurihara, Y. & Watanabe, Y. Arabidopsis micro-RNA biogenesis through Dicer-like 1 protein functions. *Proc. Natl. Acad. Sci. U. S. A.* **101**, 12753–12758 (2004).

21. Yang, Z., Ebright, Y. W., Yu, B. & Chen, X. HEN1 recognizes 21-24 nt small RNA duplexes and deposits a methyl group onto the 2' OH of the 3' terminal nucleotide. *Nucleic Acids Res.* **34**, 667–675 (2006).

22. Yi, R., Qin, Y., Macara, I. G. & Cullen, B. R. Exportin-5 mediates the nuclear export of pre-microRNAs and short hairpin RNAs. *Genes Dev.* **17**, 3011–3016 (2003).

23. Lund, E., Guttinger, S., Calado, A., Dahlberg, J. E. & Kutay, U. Nuclear export of microRNA precursors. *Science* **303**, 95–98 (2004).

24. Bohnsack, M. T., Czaplinski, K. & Gorlich, D. Exportin 5 is a RanGTP-dependent dsRNA-binding protein that mediates nuclear export of pre-miRNAs. *RNA* **10**, 185–191 (2004).

25. Zeng, Y. & Cullen, B. R. Structural requirements for pre-microRNA binding and nuclear export by Exportin 5. *Nucleic Acids Res.* **32**, 4776–4785 (2004).

26. Treiber, T., Treiber, N. & Meister, G. Regulation of microRNA biogenesis and function. *Thromb. Haemost.* **107**, 605–610 (2012).

27. Vaucheret, H., Vazquez, F., Crété, P. & Bartel, D. P. The action of ARGONAUTE1 in the miRNA pathway and its regulation by the miRNA pathway are crucial for plant development. *Genes Dev.* **18**, 1187–1197 (2004).

28. Baumberger, N. & Baulcombe, D. C. Arabidopsis ARGONAUTE1 is an RNA Slicer that selectively recruits microRNAs and short interfering RNAs. *Proc. Natl. Acad. Sci. U. S. A.* **102**, 11928–11933 (2005).

29. Bologna, N. G. *et al.* Short Article Nucleo-cytosolic Shuttling of ARGONAUTE1 Prompts a Revised Model of the Plant MicroRNA Short Article Nucleo-cytosolic Shuttling of ARGONAUTE1 Prompts a Revised Model of the Plant MicroRNA Pathway. *Mol. Cell* 1–11 (2018). doi:10.1016/j.molcel.2018.01.007

30. Wang, L. *et al.* NOT2 Proteins Promote Polymerase II-Dependent Transcription and Interact with Multiple MicroRNA Biogenesis Factors in Arabidopsis. *Plant Cell* **25**, 715–727 (2013).

31. Zhang, S., Xie, M., Ren, G. & Yu, B. CDC5, a DNA binding protein, positively regulates posttranscriptional processing and/or transcription of primary microRNA transcripts. *Proc. Natl. Acad. Sci.* **110**, 17588–17593 (2013).

32. Baek, D., Park, H. C., Kim, M. C. & Yun, D.-J. The role of Arabidopsis MYB2 in miR399f -mediated phosphate-starvation response. *Plant Signal. Behav.* **8**, e23488 (2013).

33. Li, L., Yi, H., Xue, M. & Yi, M. miR398 and miR395 are involved in response to SO2 stress in

Arabidopsis thaliana. *Ecotoxicology* **26**, 1181–1187 (2017).

34. Yamasaki, H., Hayashi, M., Fukazawa, M., Kobayashi, Y. & Shikanai, T. SQUAMOSA Promoter Binding Protein-Like7 Is a Central Regulator for Copper Homeostasis in Arabidopsis. *Plant Cell* **21**, 347–361 (2009).

35. Yant, L. *et al*. Orchestration of the Floral Transition and Floral Development in Arabidopsis by the Bifunctional Transcription Factor APETALA2. *Plant Cell* **22**, 2156 LP – 2170 (2010).

36. Denli, A. M., Tops, B. B. J., Plasterk, R. H. A., Ketting, R. F. & Hannon, G. J. Processing of primary microRNAs by the Microprocessor complex. *Nature* **432**, 231–235 (2004).

37. Gregory, R. I. *et al.* The Microprocessor complex mediates the genesis of microRNAs. *Nature* **432**, 235–240 (2004).

38. Dolata, J. *et al*. Regulation of Plant Microprocessor Function in Shaping microRNA Landscape. *Front. Plant Sci.* **9**, 753 (2018).

39. Lobbes, D., Rallapalli, G., Schmidt, D. D., Martin, C. & Clarke, J. SERRATE: a new player on the plant microRNA scene. *EMBO Rep.* **7**, 1052–1058 (2006).

40. Laubinger, S. *et al.* Dual roles of the nuclear cap-binding complex and SERRATE in pre-mRNA splicing and microRNA processing in Arabidopsis thaliana. *Proc. Natl. Acad. Sci.* **105**, 8795–8800 (2008).

41. KURIHARA, Y. The interaction between DCL1 and HYL1 is important for efficient and precise processing of pri-miRNA in plant microRNA biogenesis. *Rna* **12**, 206–212 (2005).

42. Ren, G. *et al*. Regulation of miRNA abundance by RNA binding protein TOUGH in Arabidopsis. *Proc. Natl. Acad. Sci. U. S. A.* **109**, 12817–12821 (2012).

43. Wang, Z. *et al.* SWI2/SNF2 ATPase CHR2 remodels pri-miRNAs via Serrate to impede miRNA production. *Nature* **557**, 516–521 (2018).

44. Zhao, Y. *et al.* The Arabidopsis nucleotidyl transferase HESO1 uridylates unmethylated small RNAs to trigger their degradation. *Curr. Biol.* **22**, 689–694 (2012).

45. Wang, X. *et al*. Synergistic and independent actions of multiple terminal nucleotidyl transferases in the 3' tailing of small RNAs in Arabidopsis. *PLoS Genet.* **11**, e1005091 (2015).

46. Dolata, J. *et al.* Salt Stress Reveals a New Role for ARGONAUTE1 in miRNA Biogenesis at the Transcriptional and Posttranscriptional Levels. *Plant Physiol.* **172**, 297–312 (2016).

47. Fahlgren, N. & Carrington, J. C. miRNA Target Prediction in Plants. *Methods Mol. Biol.* **592**, 51–57 (2010).

48. Mi, S. *et al.* Sorting of small RNAs into Arabidopsis argonaute complexes is directed by the 5' terminal nucleotide. *Cell* **133**, 116–127 (2008).

49. Takeda, A., Iwasaki, S., Watanabe, T., Utsumi, M. & Watanabe, Y. The mechanism selecting the guide strand from small RNA duplexes is different among argonaute proteins. *Plant Cell Physiol.* **49**, 493–500 (2008).

50. Maunoury, N. & Vaucheret, H. AGO1 and AGO2 act redundantly in miR408-mediated Plantacyanin regulation. *PLoS One* **6**, e28729 (2011).

51. Eamens, A. L., Smith, N. A., Curtin, S. J., Wang, M. & Waterhouse, P. M. The Arabidopsis thaliana double-stranded RNA binding protein DRB1 directs guide strand selection from microRNA duplexes The Arabidopsis thaliana double-stranded RNA binding protein DRB1 directs guide strand selection from microRNA duplexes. 2219–2235 (2009). doi:10.1261/rna.1646909

52. Eamens, A. L., Kim, K. W. & Waterhouse, P. M. DRB2, DRB3 and DRB5 function in a non-canonical microRNA pathway in Arabidopsis thaliana. *Plant Signal. Behav.* **7**, (2012).

53. Souret, F. F., Kastenmayer, J. P. & Green, P. J. AtXRN4 degrades mRNA in Arabidopsis and its substrates include selected miRNA targets. *Mol. Cell* **15**, 173–183 (2004).

54. Zhang, Z. *et al.* RISC-interacting clearing 3'- 5' exoribonucleases (RICEs) degrade uridylated cleavage fragments to maintain functional RISC in Arabidopsis thaliana. *Elife* **6**, (2017).

55. Branscheid, A. *et al.* SKI2 mediates degradation of RISC 5'-cleavage fragments and prevents secondary siRNA production from miRNA targets in Arabidopsis. *Nucleic Acids Res.* **43**, 10975–10988 (2015).

56. Aukerman, M. J. & Sakai, H. Regulation of Flowering Time and Floral Organ Identity by a MicroRNA and Its APETALA2-Like Target Genes. *Plant Cell* **15**, 2730 LP – 2741 (2003).

57. Gandikota, M. *et al.* The miRNA156/157 recognition element in the 3' UTR of the Arabidopsis SBP box gene SPL3 prevents early flowering by translational inhibition in seedlings. *Plant J.* **49**, 683–693 (2007).

58. Reis, R. S., Hart-Smith, G., Eamens, A. L., Wilkins, M. R. & Waterhouse, P. M. Gene regulation by translational inhibition is determined by Dicer partnering proteins. *Nat. Plants* **1**, 1–6 (2015).

59. Brodersen, P. *et al.* Widespread translational inhibition by plant miRNAs and siRNAs. *Science* **320**, 1185–1190 (2008).

60. Li, S. *et al.* MicroRNAs inhibit the translation of target mRNAs on the endoplasmic reticulum in Arabidopsis. *Cell* **153**, 562–574 (2013).

61. Wu, L. *et al.* DNA methylation mediated by a microRNA pathway. *Mol. Cell* **38**, 465–475 (2010).

62. Vazquez, F., Blevins, T., Ailhas, J., Boller, T. & Meins Jr, F. Evolution of Arabidopsis MIR genes generates novel microRNA classes. *Nucleic Acids Res.* **36**, 6429–6438 (2008).

63. Mallory, A. C. *et al.* MicroRNA control of PHABULOSA in leaf development: importance of pairing to the microRNA 5' region. *EMBO J.* **23**, 3356–3364 (2004).

64. Miyashima, S. *et al.* A Comprehensive Expression Analysis of the Arabidopsis MICRORNA165/6 Gene Family during Embryogenesis Reveals a Conserved Role in Meristem Specification and a Non-Cell-Autonomous Function. *Plant Cell Physiol.* **54**, 375–384 (2013).

65. Knauer, S. *et al.* A protodermal miR394 signal defines a region of stem cell competence in the Arabidopsis shoot meristem. *Dev. Cell* **24**, 125–132 (2013).

66. Zhou, Y. *et al.* Control of plant stem cell function by conserved interacting transcriptional regulators. *Nature* **517**, 377–380 (2015).

67. Laufs, P., Peaucelle, A., Morin, H. & Traas, J. MicroRNA regulation of the CUC genes is required for boundary size control in Arabidopsis meristems. *Development* **131**, 4311–4322 (2004).

68. Raman, S. *et al.* Interplay of miR164, CUP-SHAPED COTYLEDON genes and LATERAL SUPPRESSOR controls axillary meristem formation in Arabidopsis thaliana. *Plant J.* **55**, 65–76 (2008).

69. Mallory, A. C., Dugas, D. V, Bartel, D. P. & Bartel, B. MicroRNA Regulation of NAC-Domain Targets Is Required for Proper Formation and Separation of Adjacent Embryonic, Vegetative, and Floral Organs. *Curr. Biol.* **14**, 1035–1046 (2004).

70. Li, Y., Alonso-Peral, M., Wong, G., Wang, M.-B. & Millar, A. A. Ubiquitous miR159 repression of MYB33/65 in Arabidopsis rosettes is robust and is not perturbed by a wide range of stresses. *BMC Plant Biol.* **16**, 179 (2016).

71. He, J. *et al.* Threshold-dependent repression of SPL gene expression by miR156/miR157 controls vegetative phase change in Arabidopsis thaliana. *PLoS Genet.* **14**, e1007337 (2018).

72. Du, Q. & Wang, H. The role of HD-ZIP III transcription factors and miR165/166 in vascular development and secondary cell wall formation. *Plant Signal. Behav.* **10**, e1078955 (2015).

73. Zhao, Y. *et al.* MicroRNA857 Is Involved in the Regulation of Secondary Growth of Vascular Tissues in Arabidopsis. *Plant Physiol.* **169**, 2539 LP – 2552 (2015).

74. Si-Ammour, A. *et al.* miR393 and Secondary siRNAs Regulate Expression of the TIR1 / AFB2 Auxin Receptor Clade and Auxin-Related Development of Arabidopsis Leaves. *Plant Physiol.* **157**, 683–691 (2011).

75. Chen, Z.-H. *et al.* Regulation of auxin response by miR393-targeted transport inhibitor response protein 1 is involved in normal development in Arabidopsis. *Plant Mol. Biol.* **77**, 619–629 (2011).

76. Windels, D. *et al.* miR393 Is Required for Production of Proper Auxin Signalling Outputs. *PLoS One* **9**, e95972 (2014).

77. Mallory, A. C., Bartel, D. P. & Bartel, B. MicroRNA-directed regulation of Arabidopsis AUXIN RESPONSE FACTOR17 is essential for proper development and modulates expression of early auxin response genes. *Plant Cell* **17**, 1360–1375 (2005).

78. Guo, H.-S., Xie, Q., Fei, J.-F. & Chua, N.-H. MicroRNA directs mRNA cleavage of the transcription factor NAC1 to downregulate auxin signals for arabidopsis lateral root development. *Plant Cell* **17**, 1376–1386 (2005).

79. Gou, J.-Y., Felippes, F. F., Liu, C.-J., Weigel, D. & Wang, J.-W. Negative Regulation of Anthocyanin Biosynthesis in Arabidopsis by a miR156-Targeted SPL Transcription Factor. *Plant Cell* **23**, 1512 LP – 1522 (2011).

80. Yu, Z.-X. *et al.* Progressive Regulation of Sesquiterpene Biosynthesis in Arabidopsis and Patchouli (Pogostemon cablin) by the miR156-Targeted SPL Transcription Factors. *Mol. Plant* **8**, 98–110 (2015).

81. Sharma, D. *et al.* MicroRNA858 Is a Potential Regulator of Phenylpropanoid Pathway and Plant Development. *Plant Physiol.* **171**, 944 LP – 959 (2016).

82. He, H., Liang, G., Li, Y., Wang, F. & Yu, D. Two young MicroRNAs originating from target duplication mediate nitrogen starvation adaptation via regulation of glucosinolate synthesis in Arabidopsis thaliana. *Plant Physiol.* **164**, 853–865 (2014).

83. Barciszewska-Pacak, M. *et al.* Arabidopsis microRNA expression regulation in a wide range of abiotic stress responses. *Front. Plant Sci.* **6**, 410 (2015).

84. Li, W.-X. *et al.* The Arabidopsis NFYA5 transcription factor is regulated transcriptionally and posttranscriptionally to promote drought resistance. *Plant Cell* **20**, 2238–2251 (2008).

85. Li, W. *et al. Transcriptional Regulation of Arabidopsis MIR168a and ARGONAUTE1 Homeostasis in Abscisic Acid and Abiotic Stress Responses*. *Plant Physiology* **158**, (2012).

86. Shen, L., Liang, Z., Wong, C. E. & Yu, H. Messenger RNA Modifications in Plants. *Trends Plant Sci.* **24**, 328–341 (2019).

87. Iwanami, Y. & Brown, G. M. Methylated bases of ribosomal ribonucleic acid from HeLa cells. *Arch. Biochem. Biophys.* **126**, 8–15 (1968).

88. Dominissini, D. *et al.* Topology of the human and mouse m6A RNA methylomes revealed by m6A-seq. *Nature* **485**, 201–206 (2012).

89. Bhat, S. S., Bielewicz, D., Jarmolowski, A. & Szweykowska-Kulinska, Z. N6-methyladenosine (m6A): Revisiting the Old with Focus on New, an Arabidopsis thaliana Centered Review. *Genes* **9**, (2018).

90. Nichols, J. L. N6-methyladenosine in maize poly(A)-containing RNA. *Plant Sci. Lett.* **15**, 357–361 (1979).

91. Kennedy, T. D. & Lane, B. G. *Wheat embryo ribonucleates. XIII. Methyl-substituted nucleoside constituents and 5'-terminal dinucleotide sequences in bulk poly(AR)-rich RNA from imbibing wheat embryos*. *Canadian journal of biochemistry* **57**, (1979).

92. Zhong, S. *et al.* MTA is an Arabidopsis messenger RNA adenosine methylase and interacts with a homolog of a sex-specific splicing factor. *Plant Cell* **20**, 1278–88 (2008).

93. Luo, G. *et al.* Unique features of the m 6 A methylome in Arabidopsis thaliana. *Nat. Commun.* **5**, 1–8 (2014).

94. Růžička, K. *et al.* Identification of factors required for m6 A mRNA methylation in Arabidopsis reveals a role for the conserved E3 ubiquitin ligase HAKAI. *New Phytol.* **215**, 157–172 (2017).

95. Shen, L. *et al.* N6-Methyladenosine RNA Modification Regulates Shoot Stem Cell Fate in Arabidopsis. *Dev. Cell* 1–15 (2016). doi:10.1016/j.devcel.2016.06.008

96. Martínez-Pérez, M. *et al. Arabidopsis* m ^{6} A demethylase activity modulates viral infection of a plant virus and the m ^{6} A abundance in its genomic RNAs. *Proc. Natl. Acad. Sci.* **114**, 10755–10760 (2017).

97. Duan, H.-C. *et al.* ALKBH10B is An RNA N6-Methyladenosine Demethylase Affecting Arabidopsis Floral Transition. *Plant Cell* (2017).

98. Arribas-Hernández, L. *et al.* An m(6)A-YTH Module Controls Developmental Timing and Morphogenesis in Arabidopsis([OPEN]). *Plant Cell* **30**, 952–967 (2018).

99. Scutenaire, J. *et al.* The YTH Domain Protein ECT2 is an m6A Reader Required for Normal Trichome Branching in Arabidopsis. *Plant Cell* **30**, tpc.00854.2017 (2018).

100. Wei, L.-H. *et al.* The m(6)A Reader ECT2 Controls Trichome Morphology by Affecting mRNA Stability in Arabidopsis([OPEN]). *Plant Cell* **30**, 968–985 (2018).

101. Wan, Y. *et al.* Transcriptome-wide high-throughput deep m6A-seq reveals unique differential m6A methylation patterns between three organs in Arabidopsis thaliana. *Genome Biol.* **16**, 1–26 (2015).

102. Ok, S. H. *et al.* Novel CIPK1-associated proteins in Arabidopsis contain an evolutionarily conserved C-terminal region that mediates nuclear localization. *Plant Physiol.* **139**, 138–150 (2005).

103. Wang, Y. *et al.* N6-methyladenosine modification destabilizes developmental regulators in embryonic stem cells. *Nat. Cell Biol.* **16**, 191–8 (2014).

104. Ke, S. *et al.* m(6)A mRNA modifications are deposited in nascent pre-mRNA and are not required for splicing but do specify cytoplasmic turnover. *Genes Dev.* **31**, 990–1006 (2017).

105. David, C. J., Chen, M., Assanah, M., Canoll, P. & Manley, J. L. HnRNP proteins controlled by c-Myc deregulate pyruvate kinase mRNA splicing in cancer. *Nature* **463**, 364–368 (2010).

106. Zhao, X. *et al.* FTO-dependent demethylation of N6-methyladenosine regulates mRNA splicing and is required for adipogenesis. *Cell Res.* **24**, 1403–1419 (2014).

107. Haussmann, I. U. *et al.* m6A potentiates Sxl alternative pre-mRNA splicing for robust Drosophila sex determination. *Nature* **540**, 301 (2016).

108. Ke, S. *et al.* A majority of m6A residues are in the last exons, allowing the potential for 3' UTR regulation. *Genes Dev.* **29**, 2037–2053 (2015).

109. Molinie, B. *et al.* m6A-LAIC-seq reveals the census and complexity of the m6A epitranscriptome. *Nat. Methods* **13**, 692–698 (2016).

110. Roundtree, I. A. *et al.* YTHDC1 mediates nuclear export of N6-methyladenosine methylated mRNAs. *Elife* **6**, e31311 (2017).

111. Lesbirel, S. *et al.* The m(6)A-methylase complex recruits TREX and regulates mRNA export. *Sci. Rep.* **8**, 13827 (2018).

112. Wang, X. *et al.* N6-methyladenosine modulates messenger RNA translation efficiency. *Cell* **161**, 1388–1399 (2015).

113. Lin, S., Choe, J., Du, P., Triboulet, R. & Gregory, R. I. The m(6)A Methyltransferase METTL3 Promotes Translation in Human Cancer Cells. *Mol. Cell* **62**, 335–345 (2016).

114. Coots, R. A. *et al.* M6A Facilitates eIF4F-Independent mRNA Translation. *Mol. Cell* 1–11 (2017). doi:10.1016/j.molcel.2017.10.002

115. Mao, Y. *et al.* m6A in mRNA coding regions promotes translation via the RNA helicase-containing YTHDC2. *Nat. Commun.* **10**, 5332 (2019).

116. Anderson, S. J. *et al.* N6-Methyladenosine Inhibits Local Ribonucleolytic Cleavage to Stabilize mRNAs in Arabidopsis. *Cell Rep.* **25**, 1146-1157.e3 (2018).

117. Liu, N. *et al.* N(6)-methyladenosine-dependent RNA structural switches regulate RNA-protein interactions. *Nature* **518**, 560–564 (2015).

118. Wu, F.-H. *et al.* Tape-Arabidopsis Sandwich - a simpler Arabidopsis protoplast isolation method. *Plant Methods* **5**, 16 (2009).

119. Bodi, Z. *et al.* Adenosine Methylation in Arabidopsis mRNA is Associated with the 3' End and Reduced Levels Cause Developmental Defects. *Front. Plant Sci.* **3**, 48 (2012).

120. Zielezinski, A. *et al.* mirEX 2.0 - an integrated environment for expression profiling of plant microRNAs. *BMC Plant Biol.* **15**, 144 (2015).

121. Bielewicz, D. *et al.* mirEX: a platform for comparative exploration of plant pri-miRNA expression data. *Nucleic Acids Res.* **40**, D191–D197 (2012).

122. Roost, C. *et al.* Structure and thermodynamics of N6-methyladenosine in RNA: A spring-loaded base modification. *J. Am. Chem. Soc.* **137**, 2107–2115 (2015).

123. Liu, N. *et al.* N6-methyladenosine alters RNA structure to regulate binding of a low-complexity protein. *Nucleic Acids Res.* **45**, 6051–6063 (2017).

124. Anderson, S. J., Willmann, M. R. & Gregory, B. D. Protein Interaction Profile Sequencing (PIP-seq) in Plants. *Curr. Protoc. Plant Biol.* **1**, 163–183 (2016).

125. Foley, S. W. & Gregory, B. D. Protein interaction profile sequencing (PIP-seq). *Curr. Protoc. Mol. Biol.* **2016**, 1–20 (2016).

126. Jia, T. *et al.* The Arabidopsis MOS4-associated Complex Promotes MicroRNA Biogenesis and Precursor Messenger RNA Splicing. *Plant Cell* **2**, tpc.00370.2017 (2017).

127. Li, S. *et al.* MAC3A and MAC3B, Two Core Subunits of the MOS4-Associated Complex, Positively Influence miRNA Biogenesis. *Plant Cell* **30**, 481 LP – 494 (2018).

128. Zhang, S., Liu, Y. & Yu, B. PRL1, an RNA-Binding Protein, Positively Regulates the Accumulation of miRNAs and siRNAs in Arabidopsis. *PLOS Genet.* **10**, e1004841 (2014).

129. Chen, T., Cui, P. & Xiong, L. The RNA-binding protein HOS5 and serine/arginine-rich proteins RS40 and RS41 participate in miRNA biogenesis in Arabidopsis. *Nucleic Acids Res.* **43**, 8283–8298 (2015).

130. Kim, S. *et al.* Two cap-binding proteins CBP20 and CBP80 are involved in processing primary MicroRNAs. *Plant Cell Physiol.* **49**, 1634–1644 (2008).

131. Zhang, Z. *et al.* KETCH1 imports HYL1 to nucleus for miRNA biogenesis in Arabidopsis. *Proc. Natl. Acad. Sci. U. S. A.* **114**, 4011–4016 (2017).

132. Tang, C. *et al.* ALKBH5-dependent m6A demethylation controls splicing and stability of long 3′-UTR mRNAs in male germ cells. *Proc. Natl. Acad. Sci.* **115**, E325 LP-E333 (2018).

133. Zhou, K. I. *et al.* Regulation of Co-transcriptional Pre-mRNA Splicing by m6A through the Low-Complexity Protein hnRNPG. *Mol. Cell* **76**, 70-81.e9 (2019).

134. Wang, P., Doxtader, K. A. & Nam, Y. Structural Basis for Cooperative Function of Mettl3 and Mettl14 Methyltransferases. *Mol. Cell* **63**, 306–317 (2016).

135. Alarcón, C. R., Lee, H., Goodarzi, H., Halberg, N. & Tavazoie, S. F. N6-methyladenosine

marks primary microRNAs for processing. *Nature* **519**, 482–5 (2015).

136. Alarcón, C. R. *et al.* HNRNPA2B1 Is a Mediator of m(6)A-Dependent Nuclear RNA Processing Events. *Cell* **162**, 1299–308 (2015).

137. Bhat, S. S., Jarmolowski, A. & Szweykowska-Kulińska, Z. MicroRNA biogenesis: Epigenetic modifications as another layer of complexity in the microRNA expression regulation. *Acta Biochim. Pol.* **63**, 717–723 (2016).

138. Bielewicz, D. *et al.* Introns of plant pri-miRNAs enhance miRNA biogenesis. *EMBO Rep.* **14**, 622–628 (2013).

139. Schwab, R., Speth, C., Laubinger, S. & Voinnet, O. Enhanced microRNA accumulation through stemloop-adjacent introns. *EMBO Rep.* **14**, 615–621 (2013).

140. Köster, T. *et al.* Regulation of pri-miRNA processing by the hnRNP-like protein AtGRP7 in Arabidopsis. *Nucleic Acids Res.* **42**, 9925–9936 (2014).

141. Bajczyk, A. M. *et al.* miRNA precursors in Arabidopsis. **1**, (2020).

142. Chen, T. *et al.* M6A RNA methylation is regulated by microRNAs and promotes reprogramming to pluripotency. *Cell Stem Cell* **16**, 289–301 (2015).

143. Gosai, S. J. *et al.* Global Analysis of the RNA-Protein Interaction and RNA Secondary Structure Landscapes of the Arabidopsis Nucleus. *Mol. Cell* **57**, 376–388 (2015).

144. Liu, B. *et al.* A potentially abundant junctional RNA motif stabilized by m6A and Mg2+. *Nat. Commun.* **9**, 1–10 (2018).

145. Han, J. *et al.* METTL3 promote tumor proliferation of bladder cancer by accelerating pri-miR221/222 maturation in m6A-dependent manner. *Mol. Cancer* **18**, 110 (2019).

146. Wang, J. *et al.* METTL3/m(6)A/miRNA-873-5p Attenuated Oxidative Stress and Apoptosis in Colistin-Induced Kidney Injury by Modulating Keap1/Nrf2 Pathway. *Front. Pharmacol.* **10**, 517 (2019).

147. Xiao, W. *et al.* Nuclear m6A Reader YTHDC1 Regulates mRNA Splicing. *Mol. Cell* **61**, 507–519 (2016).

148. Morlando, M. *et al.* Primary microRNA transcripts are processed co-transcriptionally. *Nat. Struct. Mol. Biol.* **15**, 902–909 (2008).

149. Yin, S., Yu, Y. & Reed, R. Primary microRNA processing is functionally coupled to RNAP II transcription in vitro. *Sci. Rep.* **5**, 11992 (2015).

150. Fang, X., Cui, Y., Li, Y. & Qi, Y. Transcription and processing of primary microRNAs are coupled by Elongator complex in Arabidopsis. *Nat. Plants* **1**, 15075 (2015).

151. De-la-Peña, C., Nic-Can, G. I., Avilez-Montalvo, J., Cetz-Chel, J. E. & Loyola-Vargas, V. M. The Role of MiRNAs in Auxin Signaling and Regulation During Plant Development BT - Plant Epigenetics. in (eds. Rajewsky, N., Jurga, S. & Barciszewski, J.) 23–48 (Springer International Publishing, 2017). doi:10.1007/978-3-319-55520-1_2